

# Improving flood forecasting using multi-source remote sensing data together with in situ measurements

Report of the Floodfore project

**Juha-Petri Kärnä (editor), Vesa Kolhinen, Sari Metsämäki, Bertel Vehviläinen  
Timo Kuitunen, Juha Lemmetyinen, Jouni Pulliainen, Kimmo Rautiainen,  
Tuomo Smolander, Oleg Antropov, Robin Berglund, Jukka Kiviniemi, Yrjö Rauste**

NATURE  
RESOURCES





# Improving flood forecasting using multi-source remote sensing data

**Report of the Floodfore project**

**Juha-Petri Kärnä (editor), Vesa Kolhinen, Sari Metsämäki, Bertel Vehviläinen  
Timo Kuitunen, Juha Lemmetyinen, Jouni Pulliainen, Kimmo Rautiainen,  
Tuomo Smolander, Oleg Antropov, Robin Berglund, Jukka Kiviniemi, Yrjö Rauste**

Helsinki 2012

**FINNISH ENVIRONMENT INSTITUTE**



S Y K E

THE FINNISH ENVIRONMENT 12 | 2012  
Finnish Environment Institute

Layout: Seija Turunen  
Cover: YHA photo archive

The publication is available on the internet:  
[www.environment.fi/syke/publications](http://www.environment.fi/syke/publications)

ISBN 978-952-11-4001-3 (PDF)  
ISSN 1796-1637 (on-line)

## FOREWORD

FloodFore project focused on the development and implementation of new methodologies and approaches to map hydrological variables, important for the water cycle, from the combined remote sensing and in situ observation data. One objective was also to develop and demonstrate a multi-source information system as well as the use of new products as input to hydrological forecasting systems.

The project was mainly funded by TEKES, but also several Finnish companies and two ministries funded the project.

The development work was carried out by Finnish Meteorological Institute, Finnish Environment Institute SYKE and VTT. These organizations also participated in the funding of the work.

The key achievements include:

- Implementation and validation of the satellite data-aided snow (SWE) mapping system for the region of Finland. The technique has been implemented for the operational use at SYKE and is operationally assimilated to hydrological forecasting system (WSFS). The performed analysis indicates that satellite data-based SWE information is beneficial to operational hydrological forecasting.
- Implementation of the novel weather radar-based approach to map cumulative precipitation with the aid of calibration data from discrete rain gauges. The methodology is able to provide quantitative estimates e.g. on the diurnal total precipitation, which has not been possible before for the weather radar system of Finland.
- Demonstration of new satellite data-based techniques for the mapping of soil freezing in forests and bogs.
- Development and demonstration of synergistic data fusion systems in the mapping of SWE with a high resolution from the combined space-borne data sets including passive microwave (spatial resolution 25 km) and radar (spatial resolution 100 m) observations.
- Demonstration of multi-source information system for the visualization and analysis of spatially distributed multi-temporal observation/monitoring data. The demonstration system was implemented to include products on (a) weather radar-derived cumulative precipitation, (b) passive microwave satellite-derived SWE (c) optical satellite data-based fractional snow coverage and (d) WSFS hydrological model forecasts.

The developed new techniques are already in use improving the quality and performance of operational systems and services of SYKE and FMI. They may lead to new commercial applications as well (in the field of hydrological monitoring/forecasting).



## CONTENTS

<b>1 Introduction</b> .....	7
<b>2 Remote sensing products</b> .....	8
2.1 Snow Covered Area .....	8
2.2 Snow water equivalent .....	10
2.3 Cumulative precipitation .....	12
<b>3 Demonstration system</b> .....	14
<b>4 Testing satellite observations of snow covered area and snow water equivalent in hydrological forecasts</b> .....	17
Background and setup .....	17
Results .....	17
Conclusions .....	18
<b>5 Method development</b> .....	20
5.1 Combining radar and radiometer data for SWE estimation .....	20
5.2 Use of Polarimetric radar for snow estimation .....	23
Test Site and SAR Data .....	23
Snow and land cover/use data .....	24
Snow mapping technique .....	24
Polarimetric feature analysis for snow cover change monitoring .....	25
Experimental processing: snow mapping with polarimetric SAR .....	25
Dynamics of polarimetric observables during snow aggregation and melting season .....	28
Conclusion .....	30
5.3 Freeze/thaw state of the soil .....	30
Soil frost detection from active microwave observations .....	30
Soil frost detection from passive microwave observations .....	33
Algorithm development .....	33
SMOS data for regional frost detection at coarse resolution .....	34
5.4 Improving passive microwave estimates through inclusion of lake ice characteristics .....	36
<b>6 Commercialisation planning</b> .....	38
Background .....	38
Methodology and value chain .....	39
Results .....	39
Open issues and next steps .....	40
<b>7 Conclusions</b> .....	41
<b>References</b> .....	42
<b>Appendix I. Publications list</b> .....	43
<b>Documentation page</b> .....	44
<b>Kuvailulehti</b> .....	45
<b>Presentationsblad</b> .....	46

## LIST OF ABBREVIATIONS

AATSR	Advanced Along-Track Scanning Radiometer
AMSR-E	Advanced Microwave Scanning Radiometer for EOS
ASAR	Advanced Synthetic Aperture Radar
AVHRR	Advanced Very High Resolution Radiometer
CoReH2O	Cold Regions Hydrology Observatory
DEM	Digital Elevation Model
EOS	Earth Observation System
ERS-I	European Remote Sensing Satellite
ESA	European Space Agency
FF	Frost factor
FMI	Finnish Meteorological Institute
FMI-ARC	Finnish Meteorological Institute, Arctic Research
FSC	Fraction of Snow Covered Area
KML	Keyhole Markup Language
MERIS	Medium Resolution Imaging Spectrometer
MMEA	Measurement, Monitoring and Environmental Assessment
MODIS	Moderate Resolution Imaging Spectroradiometer
PNG	Portable Network Graphics
PoISAR	Polarimetric SAR
RMS	Root Mean Squared
RMSE	Root Mean Square Error
SAR	Synthetic Aperture Radar
SCA	Snow Covered Area
SMOS	Soil Moisture and Ocean Salinity
SSG	Synthetic Scenery Generator
SWE	Snow Water Equivalent
WSFS	Watershed Simulation and Forecasting System



# 1 Introduction

This report summarizes the work performed and results achieved in the FloodFore project. Project focused on the development and implementation of new methodologies and approaches to map hydrological variables, important for the water cycle at northern latitudes, from the combined remote sensing and in situ observational data. One objective was also to develop and demonstrate a multi-source information system as well as the use of new products as input to hydrological forecasting systems.

The project was mainly funded by TEKES, but also several companies, Vaisala, Astropolistieto, Kemijoki, Astrock, Metsäteho, Inergia, and Tornionlaakson Voima funded the project. Also two ministries, Ministry of Transport and Communications and Ministry of Agriculture and Forestry, gave funding.

The development work was carried out by Finnish Meteorological Institute, Finnish Environment Institute SYKE and VTT Technical Research Centre of Finland. These organizations also participated in the funding of the work (21 %). The project lasted three years, starting in November 2008 and ending in October 2011.

## 2 Remote sensing products

A principal goal of the FloodFore project was to introduce state of the art remote sensing products as an input to hydrological forecasting together with traditional in situ information in a multi-source hydrological forecasting system. For this purpose, three crucial hydrological parameters which can be measured through remote sensing were identified:

- Snow Water Equivalent (SWE); the total water content in the snowpack, affecting especially the intensity of spring flooding
- Snow Covered Area (SCA); the fractional area covered by snow, indicating the melting of snow during spring
- Cumulative precipitation; the total precipitation over a period of time
- These remote sensing products were either developed or enhanced during the project. These products were also used in the demonstration system described in section 3.

### 2.1

## Snow Covered Area

*Sari Metsämäki*

SYKE produces daily snow maps for Finland and Baltic Sea drainage area, based on visible and infrared reflectances provided by MODIS instrument onboard EOS-Terra satellite. A snow map gives the Fraction of Snow Covered area (percentage number) for grid cells of 500m × 500m in Finnish national Coordinate grid or for 3<sup>rd</sup> order sub-basins (5845 basins with average area of 50km<sup>2</sup>). Snow maps are produced using semi-automated processing; the human operation is needed for cloud mask quality check.

*SCAmod* method (Metsämäki et al. 2005) is in principal role in SYKE's snow mapping service. The method is based on the inversion of a semi-empirical model, where reflectance from target unit area is described as a non-linear combination of three reflective constituents: snow, (opaque) forest canopy and snow-free ground (snow-free forest floor underneath the tree canopy and snow-free ground in non-forested landscape). The model links those together with a) areal fractions of snow-covered terrain (FSC) and of snow-free terrain (1-FSC) and b) apparent average forest transmissivity, which describes the canopy's ability to transmit radiation, associated to a certain wavelength. Since the application area is limited to the northern latitude boreal and semi-boreal forests as well as tundra, *SCAmod*

relies on generally applicable fixed reflectance-values of the three major reflectance contributors (wet snow, dense forest canopy and snow-free ground). An essential part of the model is the apparent forest transmissivity that has to be pre-determined for each unit area. Through transmissivity, the blocking effect of the forest canopy as well as the contribution of canopy reflectance itself, are covered. Transmissivity is estimated as an inversion of SCAMod model when applied to reflectance observation made at full snow cover conditions. In principle, SCAMod is applicable to data provided operating at optical wavelengths; however, this requires tuning of the model parameters (fixed values for reflectance constituents). SCAMod has been successfully demonstrated also for MERIS and AATSR instruments onboard ESA Envisat satellite as well as AVHRR onboard NOAA satellite series. Currently, however, MODIS provides the most feasible data for daily snow map production for the area-of-interest.

After final quality check, the snow map is published in georeferenced numerical form (GeoTIFF) as well as simple picture format (PNG), with metadata attached. The whole processing chain is depicted in Figure 1.

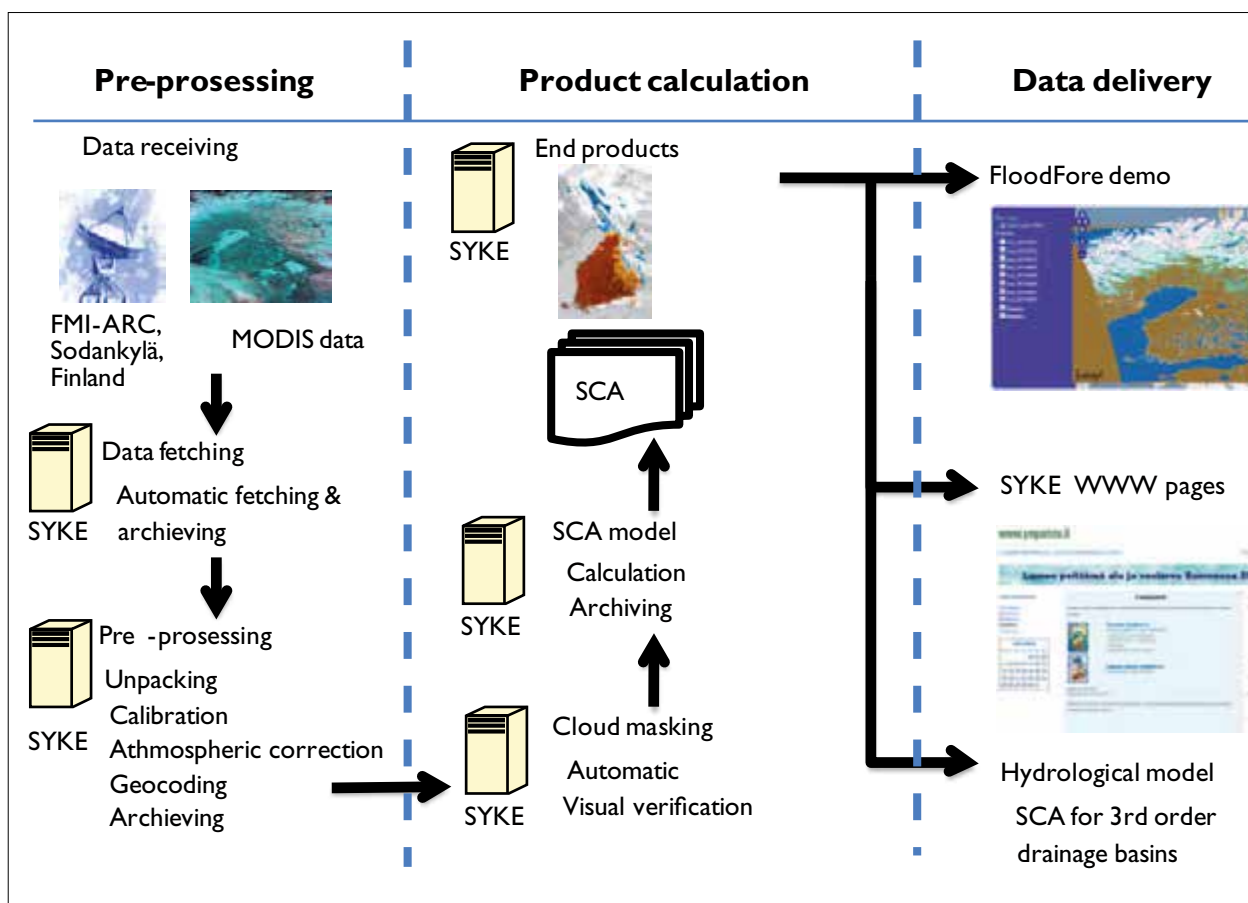


Figure 1. Processing chain of the SCA product at SYKE.

Products are mainly delivered through SYKE's web-pages ([www.environment.fi/snowcover](http://www.environment.fi/snowcover)). The snow information at sub-basin level is transferred directly to Watershed Simulation and Forecasting System (WSFS) to be used in the models. These sub-basin level products were transferred to the demonstration system during spring 2011, see Figure 2 for examples of the products.

During the FloodFore project, the SCAMod-method for snow map production was further developed in order to provide a still better accuracy. This includes 1) improvement of the transmissivity data employed by SCAMod, by inclusion of more recent MODIS-acquisitions and by increasing the number of the images and 2) employment of ground-based reflectance measurements in the determination of the values for bare ground reflectance used by SCAMod. Both these improvements also enable a more comprehensive statistical accuracy analysis which is essential when assimilating the Earth observation data into the hydrological model.

## 2.2

### Snow water equivalent

*Juha-Petri Kärnä*

Snow water equivalent (SWE) is an important hydrological parameter that tells the amount of water that would result if the snowpack would melt. It is used by the hydrological models, since it affects to the river runoffs when the accumulated snow melts.

The microwave radiometer data of AMSR-E (Advanced Microwave Scanning Radiometer for EOS) instrument in frequencies 18.7 and 36.5 GHz were used together with weather station snow depth measurements to estimate the SWE. A semi-empirical snow emission model (Pulliainen et al. 1999) was used for interpreting the passive microwave (radiometer) observations through model inversion. As a novel approach, *a priori* information of snow depth is used to calibrate the model where data are available. The basic method used in the SWE estimation is described in Pulliainen (2006) and Kärnä et al. (2007).

The overall estimation process is shown in Figure 3. First the radiometer data are acquired from a FTP server, and they are rectified to latitude-longitude coordinate system. The snow depth measurements of the weather stations from the same date are collected. Snow measurements are interpolated to cover the whole estimation area, in this case Finland. Then the assimilation method is performed using the data and snow emission model. At last, the end products are produced and published. Examples of the produced SWE estimation maps are shown in Figure 4. The SWE estimation maps are calculated in 5 km grid and then averaged to 3<sup>rd</sup> level sub basins (average size of 50 km<sup>2</sup>).

SWE estimations were produced through the spring 2010 and 2011 and they were transferred daily to the demonstration system. The operation period began on January 4<sup>th</sup> and it ended on April 29<sup>th</sup>, 2011.

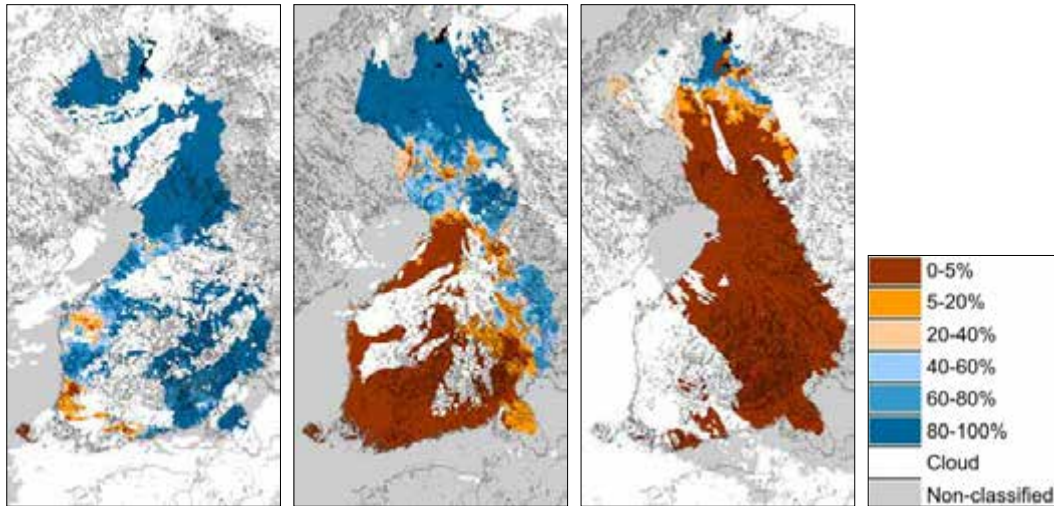


Figure 2. Sub-basin level snow covered area maps from April 16<sup>th</sup>, April 24<sup>th</sup>, and May 13<sup>th</sup> of 2011.

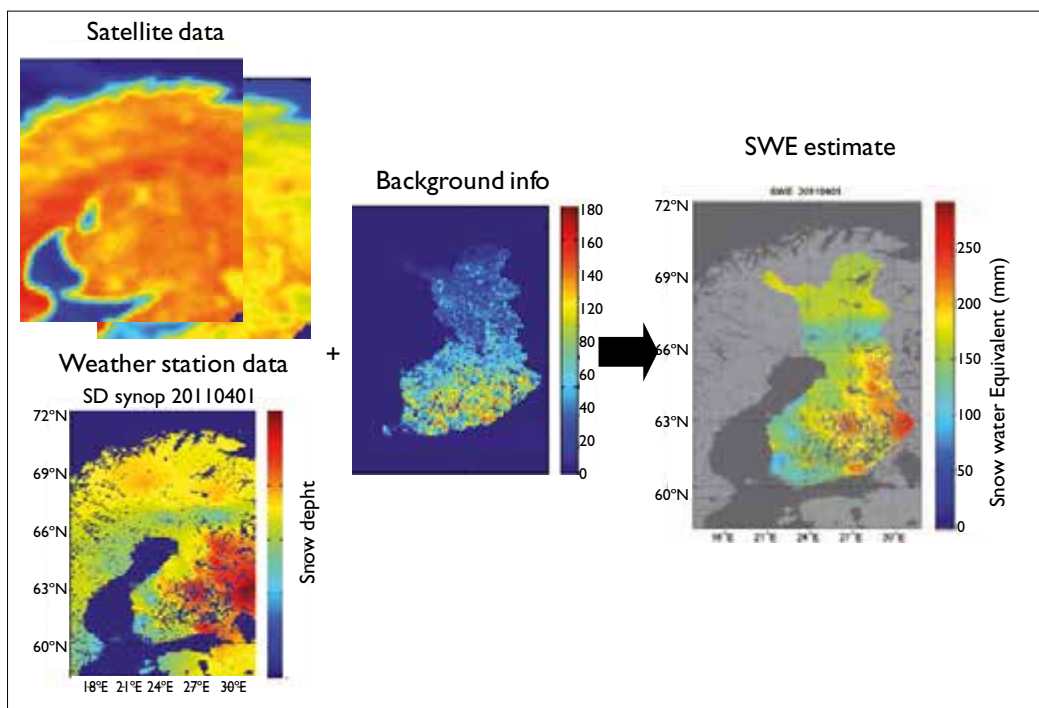


Figure 3. The SWE estimation process showing the data flow. Background info includes forest stem volume map.

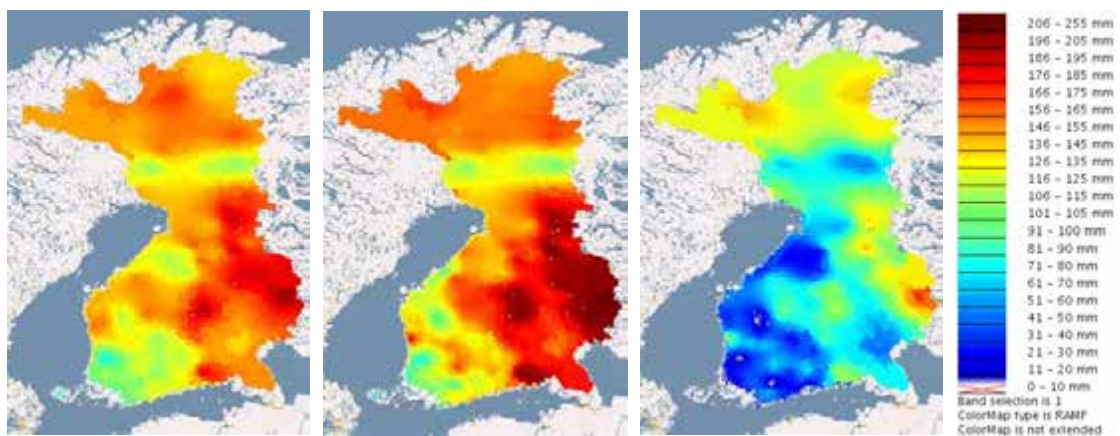


Figure 4. Snow water equivalent estimation of March 15<sup>th</sup>, April 1<sup>st</sup> and April 10<sup>th</sup>, 2011 averaged to 3<sup>rd</sup> level sub-basins.

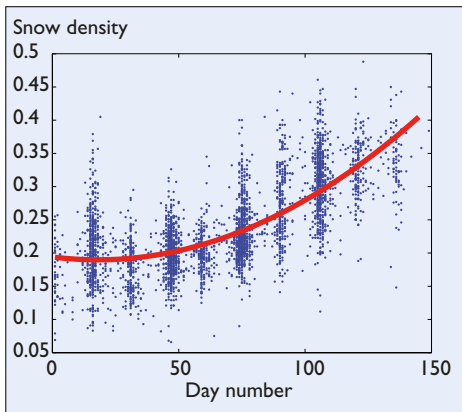


Figure 5. SYKE's snow density measurements done in 2005-2010 in Finland (blue dots) and the curve fitted to the measurements (red line).

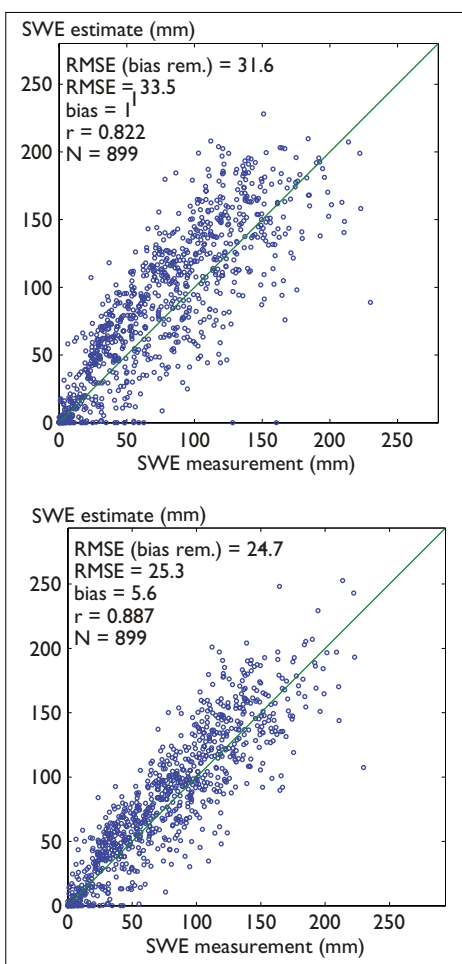


Figure 6. SWE estimates plotted versus SWE measurements from years 2007-2011: estimation done with a constant snow density (left) and with time depended snow density (right).

The method was improved in 2011 by taking into account the change in snow density during the spring. The snow density changes during the spring as shown in Figure 5. The time depended curve shown in red was added to the estimation method to have better snow density estimate.

The SWE estimation method was validated using snow course measurements of SYKE. Total of 898 SWE measurements from years 2007–2011 were used.

By using the time depended snow density instead of a constant snow density of  $0.24 \text{ g/cm}^3$ , the RMS error of the SWE estimates decreased from 33 mm to 25 mm, bias decreased from 11 mm to 6 mm, and correlation coefficient increased from 0.82 to 0.89 (see Figure 6).

### 2.3

## Cumulative precipitation

*Timo Kuitunen*

Weather radars measure precipitation every 5 minutes and we calculate twenty-four hours precipitations in 1 km grid from that data. Foundations of the measurement and calculation methods are described in Aaltonen et al. (2008).

In this project we improved still more the accuracy of precipitation measurements by calculating vertical profile corrections (VPR) every 15 minutes and making those corrections to every measurement. Principles of the VPR can be found in Pohjola (2003) and Koistinen et al. (2003).

Besides Finnish Meteorological Institute (FMI) produces hourly information about the phase of precipitation (water, wet snow, snow) in 10 km grid and we use that information too.

In order to get ground level precipitation using weather radar measurements aloft we use gauge adjustment. For each radar we take measurements and their corresponding gauge values for long enough period just before every day (e.g. 25 days or even less if there is enough rain) and calculate statistical coefficient for the correction to each radar. By using this kind of radar-gauge correction we can maintain the local structure of the radar precipitation field and get rid of errors due to different calibrations of the radars. We also make error estimates and compare the results monthly with precipitation calculated in FMI using only gauges as sources.

Next we classify daily precipitations for needs of different aims e.g. relating to catchment areas, radar measurements corresponding to each gauge, rain state statistics, hydrological models and so on. And finally we save these results in such a format that is the most suitable for those needs (ESRI ASCII, hdf5, and GeoTIFF).

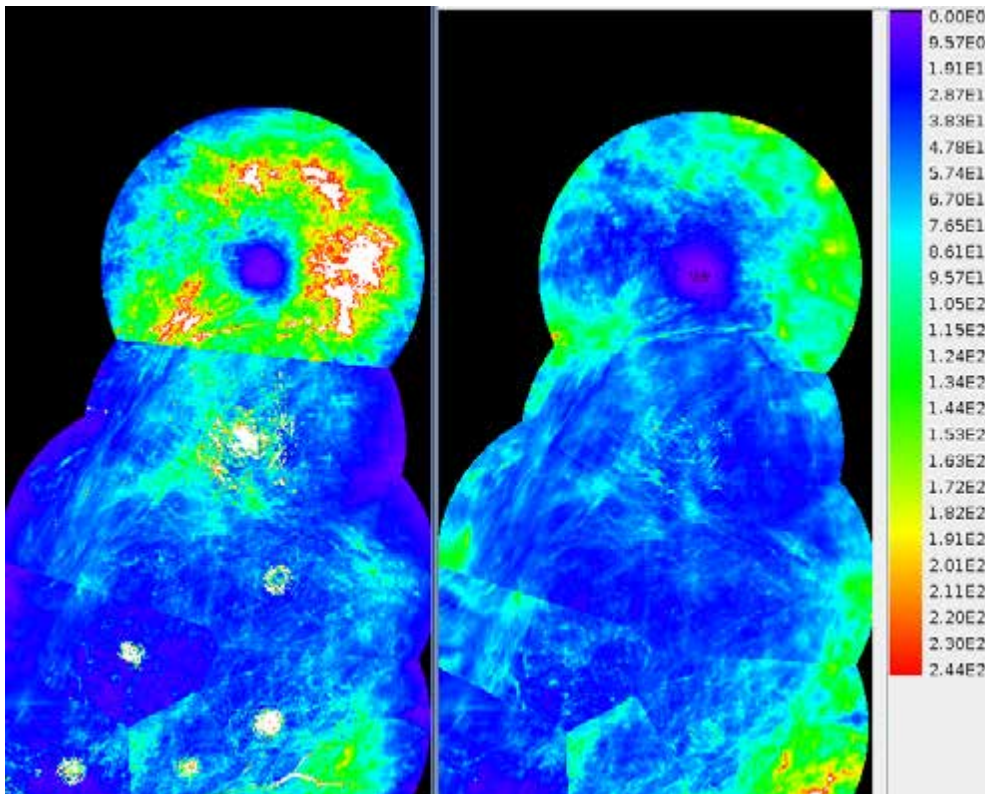


Figure 7. August 2011 precipitation in millimeters measured with Finnish weather radar network: without any corrections (left) and with all corrections described above (right).

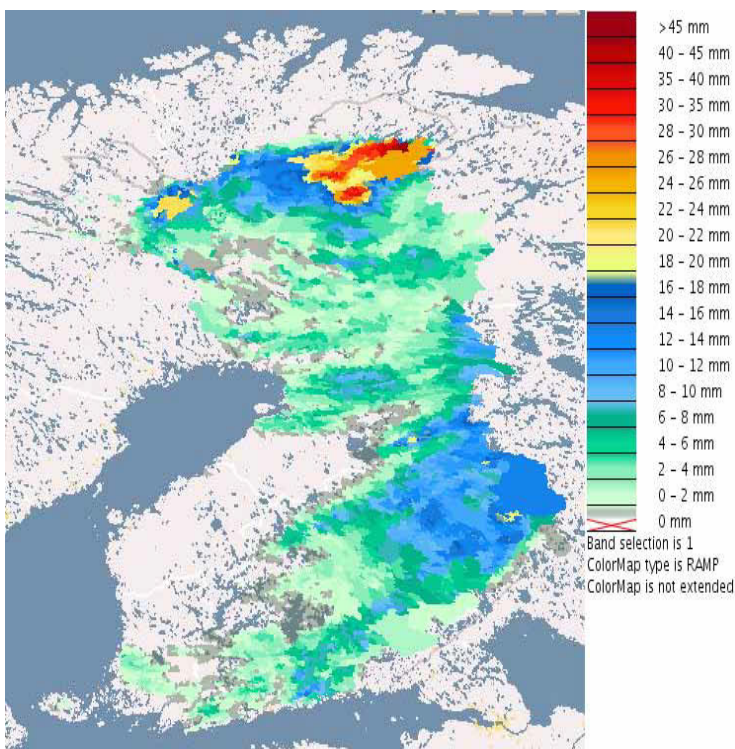


Figure 8. Cumulative 24 h precipitation on September 1<sup>st</sup>, 2010 calculated for 3<sup>rd</sup> level sub basins.

### 3 Demonstration system

*Robin Berglund*

The first prototype of the demonstration system was implemented based on Google Earth, which provides easy to use viewing functions like panning and zooming and is able to show different layers of data over base map. This simple approach was also used as one of the tools when gathering user requirements during a workshop organized during the first year of the project.

After a requirements study phase a demonstration system was implemented as an application running on a server hosted by VTT and accessible via a web browser. The reason for choosing this approach was to be able to demonstrate to a group of users a set of interactive operations that were not feasible to implement using just simple viewing tools like Google Earth.

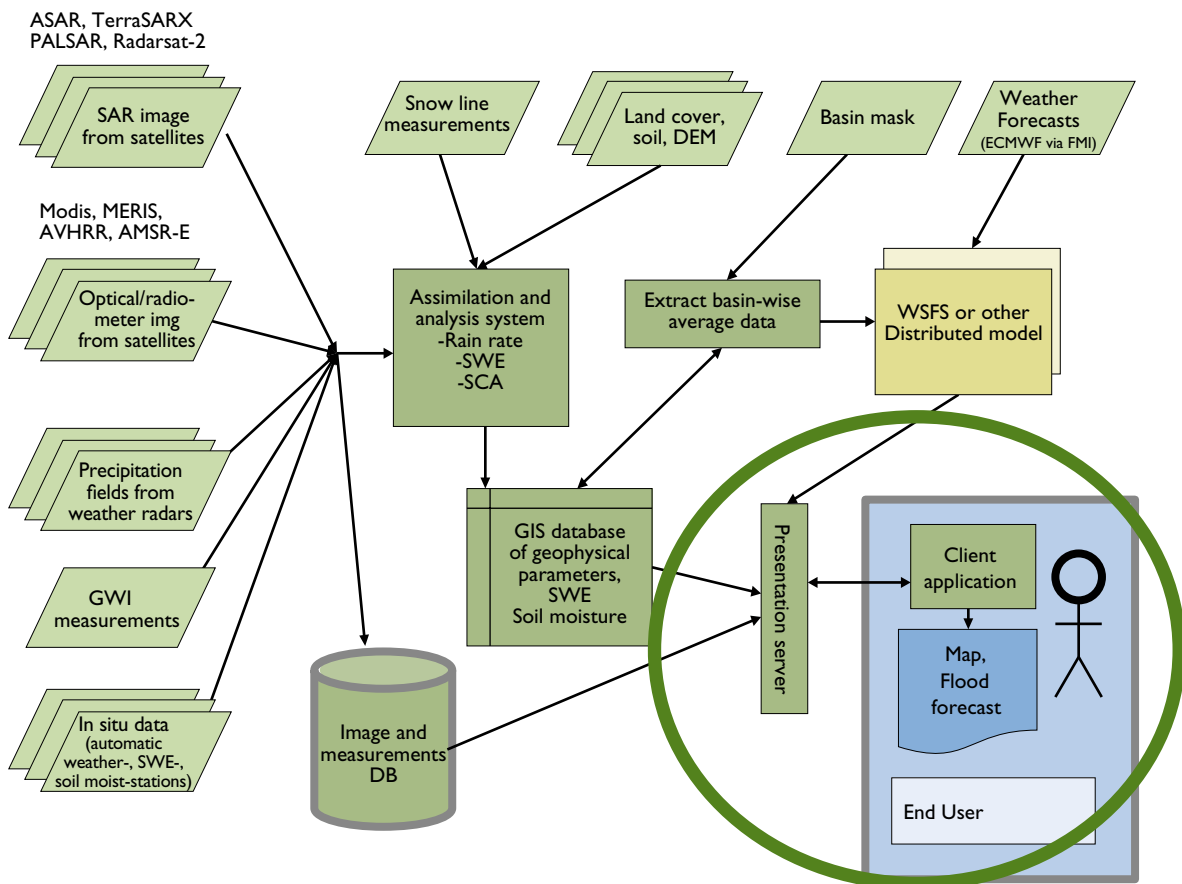


Figure 9. The prototype demonstration system is enclosed in the green ellipse.



The main functionality was to enable the user to view a limited number of product types as overlays on a map. The product types were Snow Covered Area (SCA), Snow Water Equivalent (SWE) and cumulative precipitation. Also several fully polarimetric (quad-polarization) SAR images in Pauli basis representation were included as examples. The main products (SWE and SCA) are automatically fed into the system – as soon as the image products are pushed from SYKE to VTT, the system ingests the products and enables the user to select these for display in the browser window.

The demo system contains a set of functions selected during the User workshop. The most important ones are:

- display of **numerical values** of the products at a point currently visible on the map
- display of **time series** of values as a graph at an interactively given point on the map for different products
- display of **values as a graph** along an interactively drawn **line**
- display of an estimate of the **average value** within an interactively drawn **polygon** for all visible products as a graph.

The demo system also enables the user to export the selected layers as KML files with time stamps included. This makes it possible to use Google Earth as a viewer of the selected products and in that way visually integrate other location based information (roads, borders, towns, etc..) with the FloodFore products.

The implementation is based on open source components such as GeoServer, OpenLayers and Javascript libraries. The metadata of the products is included in the filenames that adhere to an agreed naming convention. This is not the best way to go as a generic approach, but served the requirements of this project sufficiently.

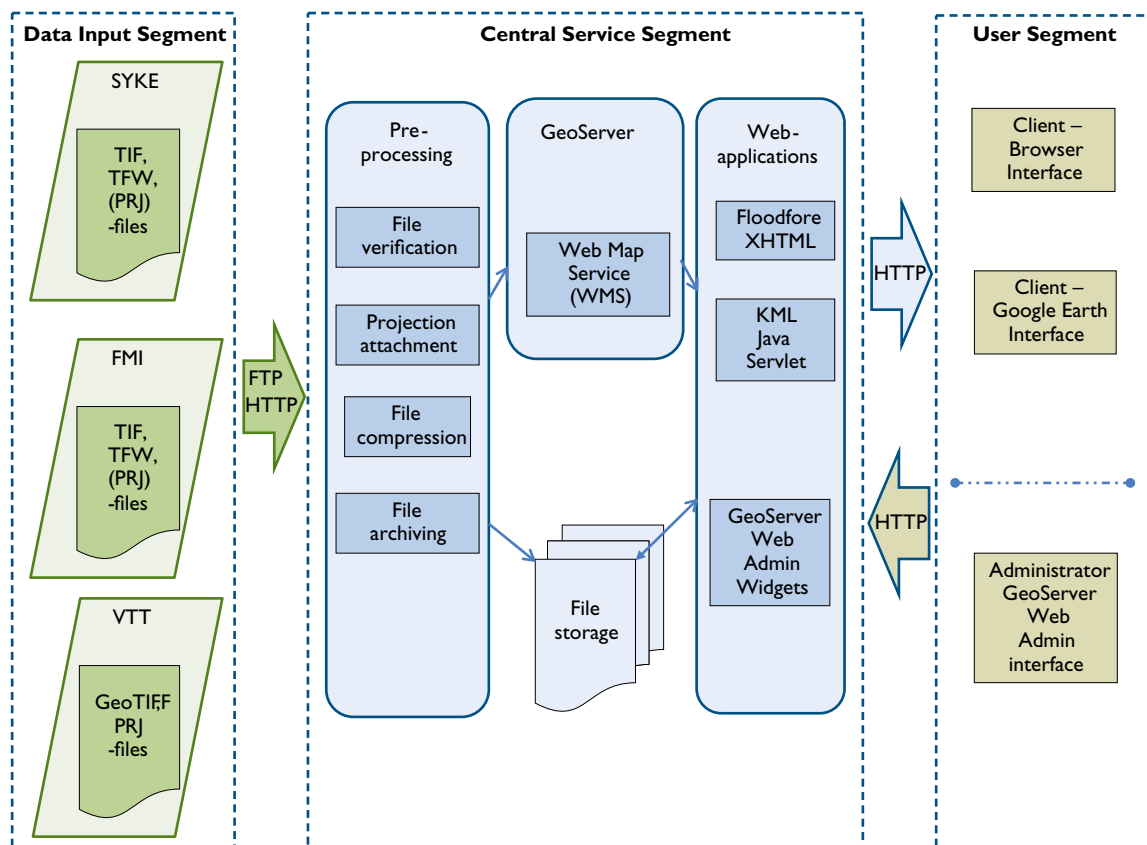


Figure 10. Elements in the demonstration system.

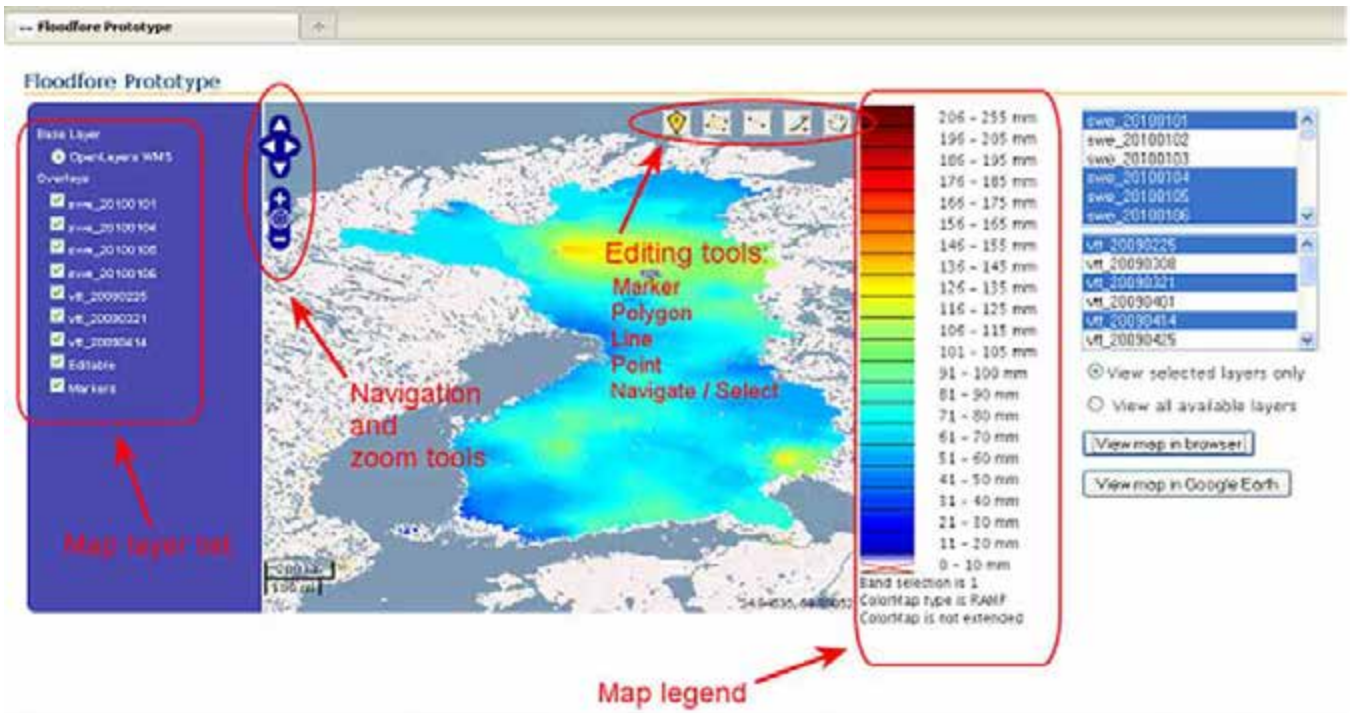


Figure 11. User interface of the prototype demonstration system.

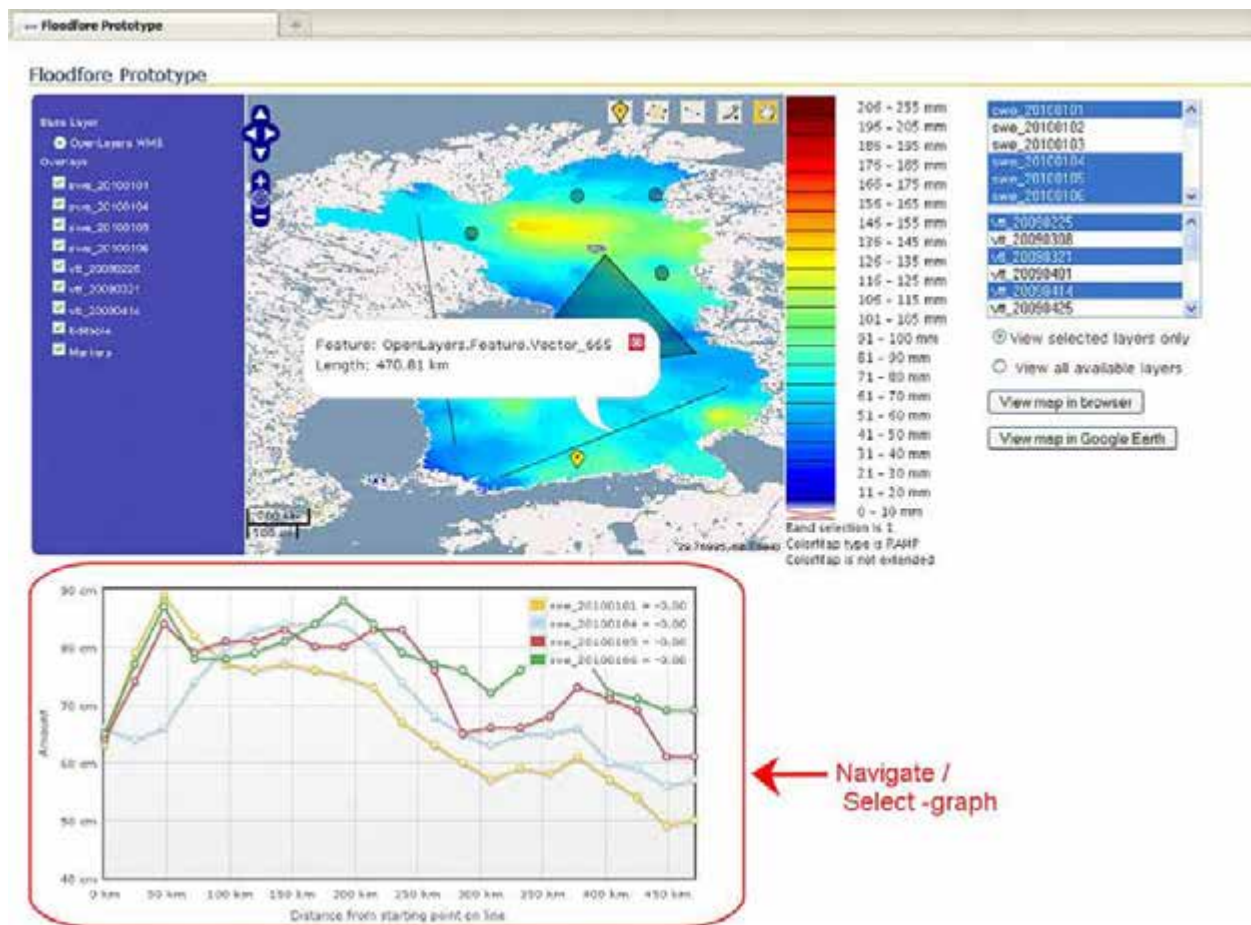


Figure 12. Example of the graphs displayed in the demonstration system.

# 4 Testing satellite observations of snow covered area and snow water equivalent in hydrological forecasts

*Vesa Kolhinen & Bertel Vehviläinen*

## Background and setup

In order to study how the satellite borne snow covered area (SCA) estimates and snow water equivalent (SWE) values affect on the accuracy of hydrological forecast made by the hydrological model of Watershed Simulation and Forecasting System (WSFS), a set of tests were conducted for Kemijoki river basin in the Northern Finland. WSFS simulates hydrological cycle with quantities such as water level and discharge. Simulated discharge is routinely corrected using (real time) discharge observations when available. Utilization of satellite snow observations were now tested to update the forecasts and to determine whether they could provide additional information and accuracy especially during the spring season forecasting.

Test period reached from April 15, 2009 to June 10, 2009. This time interval covers the entire snow melt season: In the beginning of the period snow cover was 100 % and at the end of it snow cover had completely disappeared.

Weather data used in the 'test forecasts' were actual year 2009 data for the simulation period before forecast starting date, and after that randomly chosen weather data from years between 1962 and 2010 as 'weather forecast' starting when observation period ceases. Random historical data were chosen because the actual old weather predictions were not available. Weather forecast based on data of previous years increase the uncertainty of predicted discharge.

Forecast simulations were run with and without satellite SCA and SWE observations. Several discharge observation points: LUIRO Kammonen, Kokkosniva, KÖNGÄS (Ounasjoki), Marraskoski (Ounasjoki), Valajaskoski, Kemijärvi and Savukoski were used for these forecast simulations as 'real time' observations for updating.

## Results

After the first forecast test simulations it was observed, that WSFS calculates discharge well enough without additional information from satellite observations of SCA and SWE. Therefore, an artificial 40 % error was introduced into precipitation observation and thus also into the estimated snow water equivalent. This provided a method to see how well and how quickly satellite snow observations correct the test forecast.

To gain an overall view of the effects, we plotted the incoming discharge sum over the simulation and test forecast period of each run, which include discharge simulation first with observed weather data and after the forecast starting date as 'forecasted weather'. In other words, simulated discharge over the entire period including observation and forecast period was calculated for each test forecast day. These are plotted and compared to the observed sum over the period.

It turns out that results vary in different simulation points in the Kemijoki catchment. Ideally, the normal test simulations without any additional precipitation error would coincide with the observed results, and the cases with precipitation error would gain advantage of satellite measurements and be corrected towards observation during simulation. This happens at Luiro Kammonen and also at Kokkosniva, although not that clearly.

Results of forecast simulations for Luiro Kammonen are presented in Figure 13, where discharge sums in both cases (observed precipitation and +40 % error in precipitation) are plotted as a function of forecast day for each three scenarios: SCA observations used for correction, SWE observations used for correction and no satellite observations in use. Figure clearly shows that normal forecast simulation without satellite observations matches well with the discharge observations, and that no additional benefit is obtained from SCA and SWE observations.

The case of artificial 40 % increase in precipitation is shown in the same figure. The effect of SCA and SWE observations are now readily seen from the figure: SWE satellite observation guided simulation is corrected immediately at the beginning of the test simulation/forecast, and the results goes close to the observed discharge sum. This is because satellite SWE observations are available and provide additional information of correct SWE from the very beginning of the period. SCA observations, on the other hand, begin to provide additional information only when snow begins to melt and SCA starts to decrease. This is seen to happen around May 10–15th, as simulations using SCA observations begin to converge towards observed discharge sum. Finally, the reference case without satellite observations matches the observed values only at the end of the simulation/forecast period, when discharge observations guide the model towards the correct water volume or discharge sum.

The other simulation test points are more difficult to interpret. For example at Kemijärvi and Kõngäs normal simulations/forecasts miss the measured results in the beginning. However, SWE observations bring in both normal and 40 % error case simulations/forecast close together from the very beginning and the results are similar regardless of the precipitation accuracy and possible errors in snow water equivalent. It can be concluded, that regardless of the error in precipitation, SWE observations correct simulations/forecast immediately, although in this case to equally wrong values compared to discharge measurements.

## Conclusions

It appears that spring discharge forecast can be improved using satellite SWE measurements, although the effect cannot be detected when snow line measurements and precipitation measurements are available. However, these satellite observations could be used to improve simulations in the areas where snow line measurements are not available.

Satellite SCA measurements do not provide as much improvement into the simulations as SWE observations. They do improve forecast results in some areas during the period when snow coverage decreases rapidly, but generally SWE information is more useful.

Finally, snow line ground measurements are still needed in order to check seasonally that satellite observations are valid, as there might be some systematic error due to calibration, system failure, sensor change, etc.

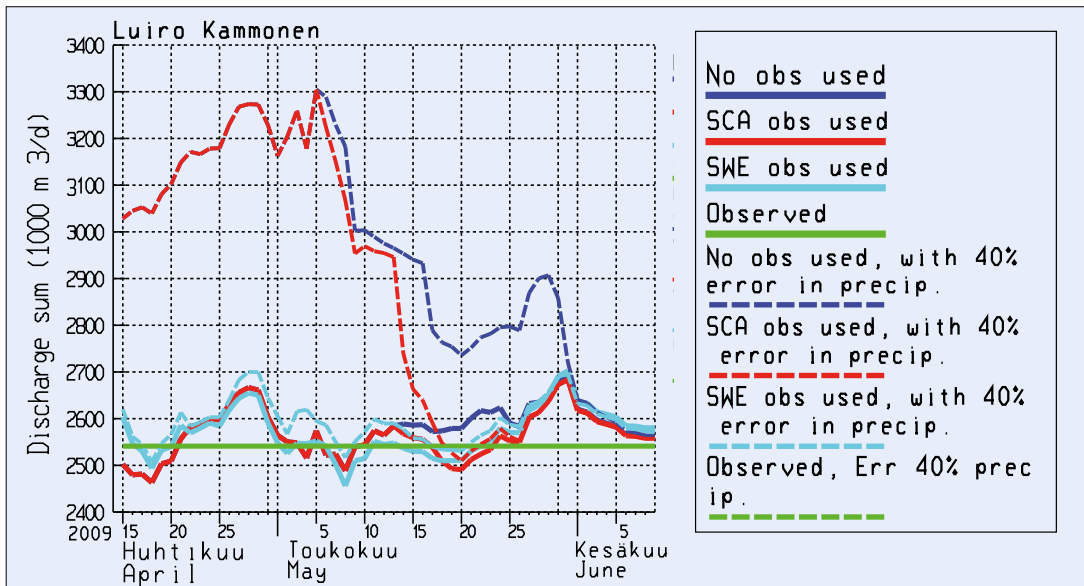


Figure 13. Luiro Kammonen: Simulated/forecasted and observed discharge sums (over the whole test period) are plotted as a function of forecast starting time for without (solid lines) and with 40 % error in precipitation (dotted lines). In case of correct precipitation simulations with no satellite observations (blue line) as well as those with SCA (red line) and SWE observations (cyan line) match well to observed discharge sum (green line). Effects of SWE and SCA observations are seen in the case of 40 % error in precipitation: Simulation/forecasts utilizing SWE observations (cyan line) are corrected immediately at the beginning of the test period (15th April) as additional SWE information is already available and those using SCA (red line) are corrected when snow begins to melt around May 10-15th.

## 5 Method development

The FloodFore project explored novel remote sensing methodologies to detect soil and snow cover properties from space. The conducted work included a possible enhancement to the SWE product, novel methodologies to detect snow cover properties from SAR (Synthetic Aperture Radar) observations, and methodologies to detect the soil freeze/thaw state.

### 5.1

#### Combining radar and radiometer data for SWE estimation

Juha Lemmetyinen

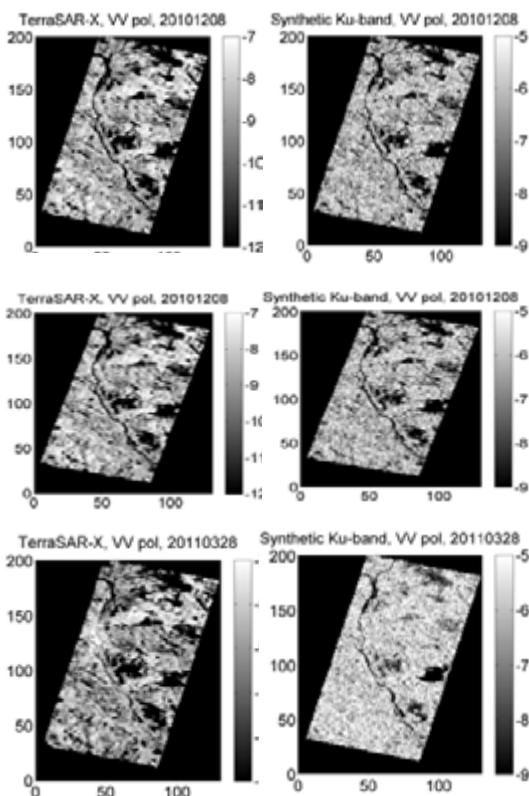


Figure 14. Three examples of X and Ku band image pairs used for retrieval (Dec 8th, 2010, Feb 1st, 2011, Mar 28th, 2011). X band images TerraSAR-X observations aggregated to 200 m resolution. Ku band images are synthetic images constructed using FMI Synthetic Scenery Generator for SAR images.

As a part of *FloodFore*, studies for employing high-resolution SAR imagery to estimate Snow Water Equivalent at high resolution were made. The investigation was made in anticipation of possible future satellite missions, i.e. the candidate ESA Earth Explorer 7 *CoReH<sub>2</sub>O* (*Cold Regions Hydrology Observatory*) mission, currently undergoing Phase A evaluation studies. The proposed mission would carry a dual polarization SAR at X and Ku bands. The mission has the potential of greatly increasing the quality, and in particular, the spatial resolution of available EO data on snow cover properties such as SWE.

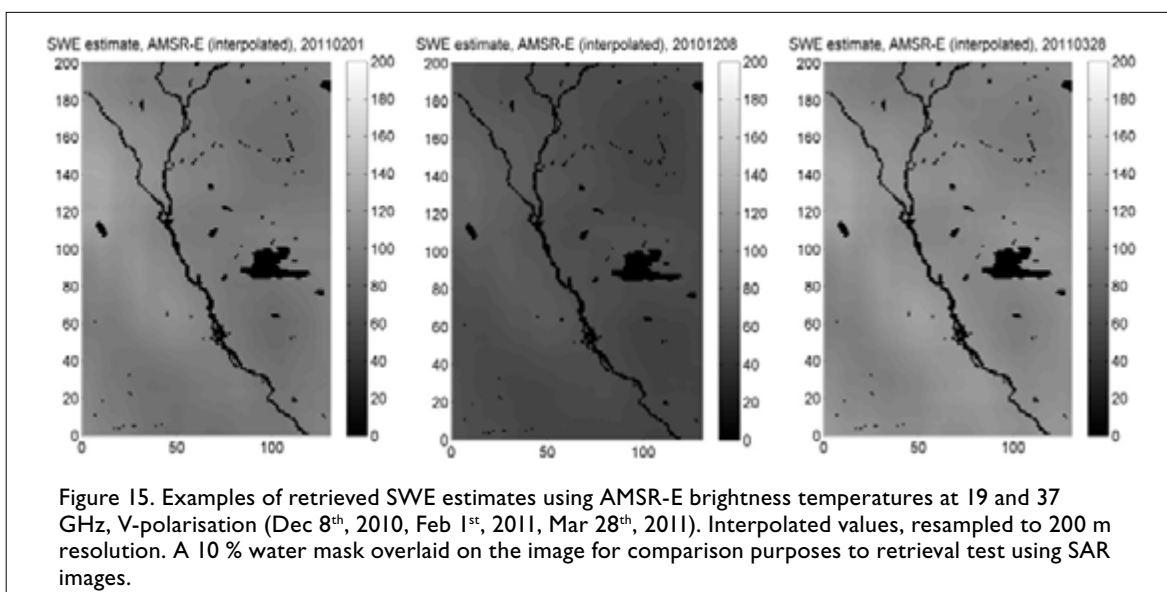
In the investigation, data from existing SAR missions was applied together with simulated data in order to study and demonstrate the potential of the mission in the retrieval of snow properties at high resolution. For this purpose, a time series of *TerraSAR-X* observations at X band (9.6 GHz) were acquired over the FMI-ARC Sodankylä site for the winter 2010–2011. However, the X band observations are not very sensitive to increasing snow volume (i.e. SWE); for this purpose, *CoReH<sub>2</sub>O* employs a second, higher frequency at Ku band. Current satellite mission do not, in fact, support Ku band SAR instruments. Therefore, for the purposes of this study, simulated images at Ku band were applied using a SSG (Synthetic Scenery Generator) developed at FMI.

Figure 14 shows three exemplary image pairs over the Sodankylä region (*TerraSAR-X* observation and synthetic Ku band image) at VV polarization for the winter 2010–2011. The synthetic Ku band images were constructed based on the *TerraSAR-X* observation, applying the SSG for transfer into the higher Ku band. A level of noise was added to the images to simulate SAR speckle effects. A total of 11 image pairs were thus acquired/created for investigation.

The actual retrieval method applied follows the SWE retrieval method already used for passive data (see section 2.2); i.e. a forward model, describing in this case backscatter from snow covered terrain, is iteratively matched to observations (in this case, SAR images) using SWE as a free parameter in the model. The end result is a SWE map at the high resolution of the model. However, SAR images typically exhibit a large level of speckle (noise). This results in a “noisy” estimate of SWE when using SAR images alone for retrieval. As a consequence, the available passive microwave data used already to produce the *FloodFore* SWE product were used in a common retrieval algorithm with the SAR data to regulate and diminish speckle effects. In essence, the passive microwave observations regulate the overall level of the obtained SWE, while the high-resolution SAR images introduce spatial variability to the estimates.

Figure 15 shows an example of typical coarse resolution passive microwave SWE estimates (in fact, the primary SWE product used in *FloodFore*). A water mask is superimposed on the images (lake Orajärvi seen to the right of the image). In comparison, SWE estimate maps for the same dates using SAR images together with the passive microwave AMSR-E observations are shown in Figure 16. Spatial features, such as open bogs with lower SWE compared to surroundings, can now be seen in the images. Also, the images demonstrate the level of variability in SWE, caused by noise, in the SAR image.

A time series comparison of both retrieval methods against *in situ* data from the FMI-Sodankylä station is demonstrated in Figure 17. The *in situ* data are from snow course surveys in the area, which cover the most common land cover categories in the area (forested areas on mineral soil, and peatbogs). In the test case, the passive estimate method can be seen to overestimate the SWE value in particular for the midwinter season, when compared to *in situ* information. This is a typical feature of the passive retrieval method. The blended SWE estimate using SAR images together with the AMSR-E observations, however, shows a considerably better match with *in situ* data. However, one advantage of the passive data is clearly visible. The data are available daily, while the SAR-based retrieval in this case was tied to the 11-day repeat-pass cycle of TerraSAR-X. The same comparison is also demonstrated as scatter plots in Figure 18; here, the SAR-based retrieval is shown as separated by land cover category. It can be seen that the demonstrated technique has the potential of improving retrieval accuracies in particular for non-vegetated areas. Vegetation (forests) forms a greater challenge for interpretation of SAR images compared to the passive microwave case, and the forward models describing backscatter from vegetation are still in development.



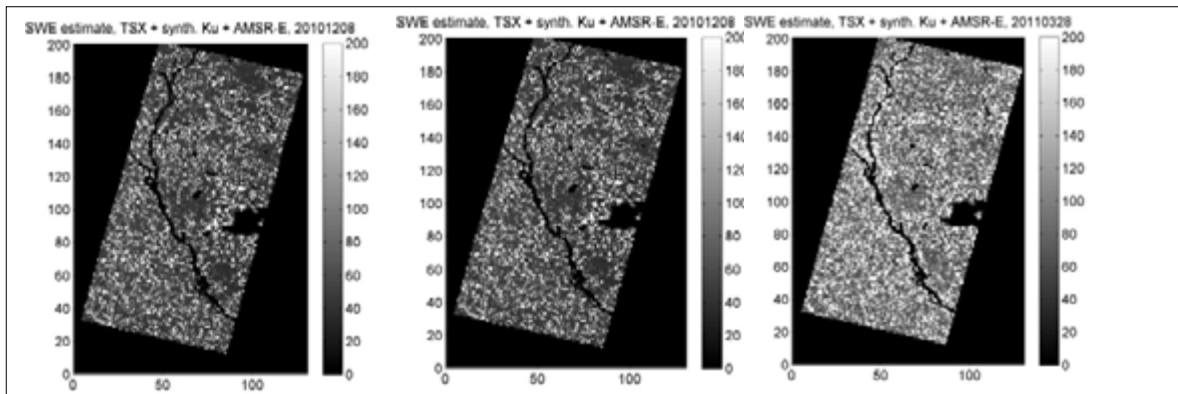


Figure 16. Examples of retrieved SWE estimates using TerraSAR-X, synthetic Ku band images and AMSR-E brightness temperatures at 19 and 37 GHz, V-polarisation (Dec 8th, 2010, Feb 1st, 2011, Mar 28th, 2011). Areas with more than 10 % of water surface masked.

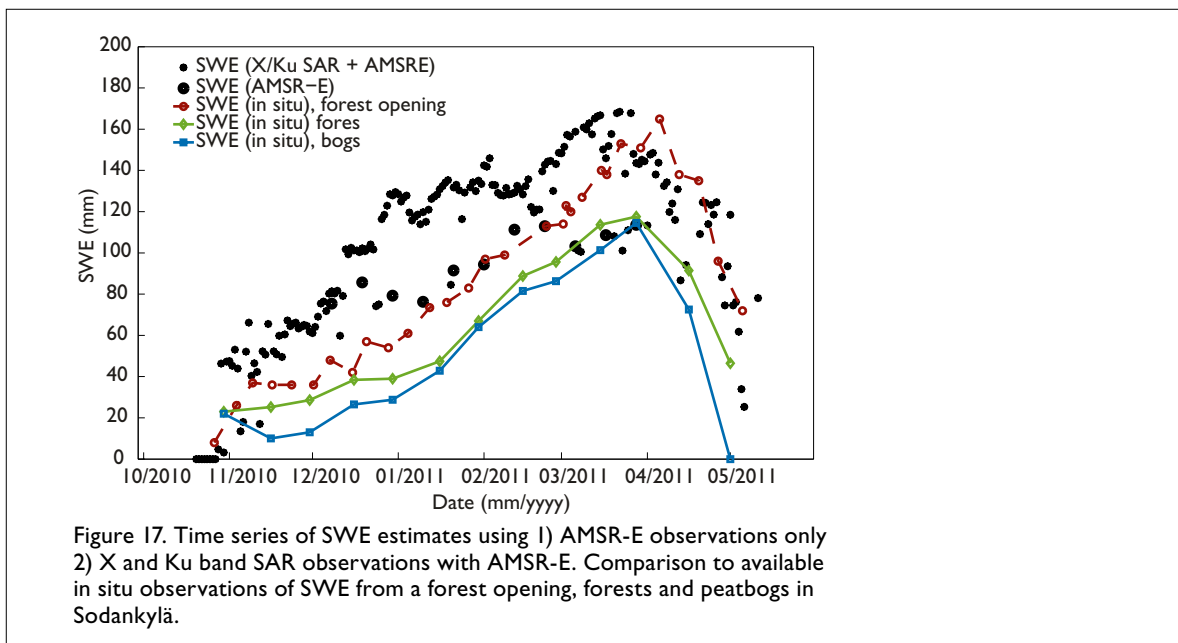


Figure 17. Time series of SWE estimates using 1) AMSR-E observations only 2) X and Ku band SAR observations with AMSR-E. Comparison to available *in situ* observations of SWE from a forest opening, forests and peatbogs in Sodankylä.

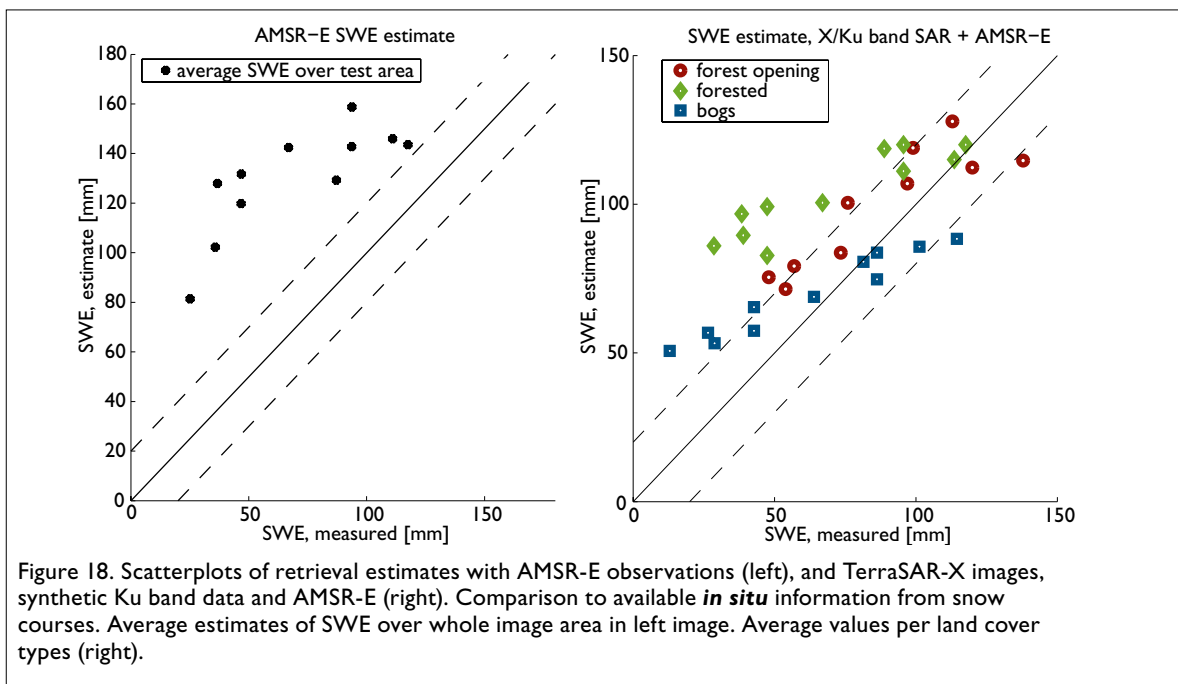


Figure 18. Scatterplots of retrieval estimates with AMSR-E observations (left), and TerraSAR-X images, synthetic Ku band data and AMSR-E (right). Comparison to available *in situ* information from snow courses. Average estimates of SWE over whole image area in left image. Average values per land cover types (right).



## Use of Polarimetric radar for snow estimation

*Oleg Antropov & Yrjö Rauste*

Use of SAR information for mapping of snow covered area (SCA) has been adopted on a regular basis in Finland for more than a decade, motivated by all-weather all-season capabilities of imaging radar. SAR data provided by ERS-1 and RADARSAT-1 satellite sensors was used as a basis for production of snow covered area maps (Koskinen et al. 1997) to be further supplied as an input to advanced hydrological and climatological models and for general environmental monitoring purposes.

The modern generation of space borne-sensors is capable of providing fully polarimetric SAR (PolSAR) data, which can be potentially related to a number of snow pack parameters, e.g. Shi et al. (1994). These include snow density, snow depth, liquid water content, snow pack roughness, and average snow grain size. Respective studies mostly used data obtained from airborne SAR campaigns, while application focus is shifting to space borne SAR information. Particular SAR sensors of interest for snow monitoring are C band RADARSAT-2 and X band TerraSAR-X. Generally, operational use of a snow mapping remote sensing system requires an extensive temporal and/or spatial coverage, which is hard to implement on a regular basis using PolSAR data from currently available sensors. However, a user can potentially benefit in increased accuracy of snow mapping methods and retrieved snow parameters from PolSAR data, as well as from qualitative interpretation of snow pack condition (Trudel et al. 2009) when compared to traditional use of single-polarization SAR data.

The objective of this section is to evaluate the potential and utility of multi-polarization SAR in snow covered area estimation and develop and to test several applicable snow-mapping techniques.

### Test Site and SAR Data

The study site was situated in Sodankylä in the vicinity of the Arctic Research Centre of FMI. The central coordinates of the test site were 67°18' N, 26°40' E. The site represents a typical sub-Arctic boreal forest zone, with seasonal snow cover lasting more than five months. Dense and sparse forests cover majority of the area, with some considerable areas of peat land and open bogs also present. A time series of 10 RADARSAT-2 images covering the study area were acquired (in the context of SOAR project 4071) during the snow melting season in February-June 2009, using two incidence angles, with five scenes each. The corresponding incidence angles were 24.6 and 38.4 degrees. The original single look complex PolSAR images have a pixel spacing of 4.7 m along track (azimuth) and about 4.7 m cross track (slant range). The timeline of image acquisition covered both dry snow season (February 25th, March 8th, March 21st, April 1st), snow melting (April 14th, April 25th, May 8th and May 19th) and snow-free season (June 1st and June 12th).

All the PolSAR imagery was ortho-rectified and radiometrically corrected using digital elevation model (DEM) with in-house VTT ortho-rectification software (Rauste et al. 2007), converting the original RADARSAT-2 products in the full scattering matrix form to radiometrically normalized multi-look SAR data in the coherency matrix file format of the ESA PolSARpro software, with pixel spacing of 25 m. The obtained geometrical accuracy was better than half a pixel, allowing application of change detection techniques.

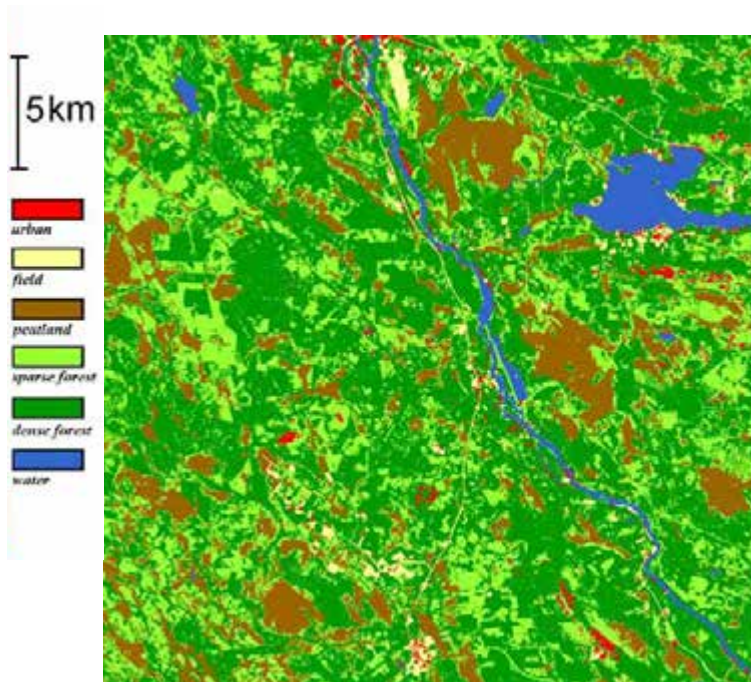


Figure 19. Land cover/use map.

## Snow and land cover/use data

For quantitative assessment of the obtained SCA maps several reference snow maps produced from Terra MODIS sensor data were used. The snow map estimates were provided by SYKE, covering the period between April, 1st and May, 20th. Spatial resolution of the snow maps was 500 m, representing percentage value of SCA in each resolution cell. For those days when extensive cloud coverage makes reasonable comparison impossible, a linear interpolation of snow coverage between neighboring dates was performed in order to obtain some reference estimate.

For monitoring polarimetric feature dynamics over different land cover classes the Finnish national part of CLC 2000 land cover/use data was used. The original land cover database of Finland was produced by SYKE and included 44

available classes (Härmä et al. 2004) with 25 m resolution. For detailed analysis of PolSAR signatures change we used only 12 most spatially significant classes (also excluding water surfaces), representing more than 96% of the scene. The land cover/use map is shown in Figure 19, with the available land cover/use classes merged to 6 land cover/use super-classes in this representation, namely urban areas, sparse forest, dense forest, agriculture and field, peat-land and open bogs, and water surfaces.

## Snow mapping technique

As a basis for the algorithm the so-called single-reference-image SCA mapping method was adopted (Nagler & Rott 2000). The algorithm for mapping wet snow applies change detection using ratios of wet snow versus snow-free (bare ground) or dry snow surfaces. The original validity measures for incidence angles were 17-78 degrees, well-fitting the available SAR imagery.

At the first stage of the algorithm, a reference image is chosen from the set of available SAR scenes acquired during either snow-free or dry-snow season. Several options for the choice of a reference image are available, with using averaged dry-snow images, bare-ground images or composite of those. As the original algorithm was developed for use with single-polarization SAR, a choice of optimal polarization or combination of these was another problem to solve. Also span polarimetric image can be used, representing combined total backscattered power and contributing to speckle reduction in SAR imagery.

Further, a ratio between the processed SAR image and the chosen reference image is calculated on a pixel by pixel basis. A predefined detection threshold is applied to this ratio afterwards, in order to discriminate between wet snow and bare ground areas and produce a wet snow cover map. As it will be of binary nature, the final fractional wet snow coverage estimate is obtained using statistics of pixels in rectangular spatial windows. These spatial windows can be either non-overlapping or can overlap, contributing to a more smooth snow map with higher spatial resolution in the latter case.

All the images to be eligible for the processing should be acquired in the same imaging geometry, ortho-rectified and radiometrically corrected. This puts some

limitations on aggregative use of time series, as e.g. incidence angle is expected to be the same for the whole set of images. In particular case of this study, it requires a separate processing of images with the incidence angle of 28.6 and 38.4 degrees. Technically, the main steps included geocoding, co-registration and ortho-rectification of images, speckle reduction, and ratio images calculation and thresholding as described above. The original method used a threshold of -3 dB to separate wet snow from other surfaces. Later studies, specifically in the boreal forest zone, reported slightly different results, with optimal threshold ranging between -1.4 dB and 0.0 dB specified for a single-reference snow mapping algorithm (Luojuus et al. 2009).

Particular points of interest included choice of optimal polarization, threshold ratio and sets of reference images, using fitting of SAR observations to snow maps derived from optical data. It is assumed, that the estimated optimal configuration can be further used as a basis for snow mapping under approximately the same environmental conditions.

### **Polarimetric feature analysis for snow cover change monitoring**

The use of PolSAR decompositions gains more attention in recent snow-mapping literature, revealing potential to relate observed change in scattering mechanisms to an actual change in snow cover state. The two most widely used incoherent decomposition techniques for natural and spatially distributed targets are the Cloude-Pottier and the Freeman-Durden decompositions.

The first technique is based on eigendecomposition of the polarimetric coherency matrix (Cloude & Pottier 1997). It uses such polarimetric characteristics for description of target properties as entropy and averaged alpha angle. Entropy  $H$  is a measure of randomness of the scatterer and covers dynamic range from 0 to 1, from deterministically polarized scatterer to isotropically depolarized scatter. Alpha angle  $\alpha$  is the averaged backscatter angle with values from  $0^\circ$  for backscatter from a single smooth surface to  $90^\circ$  for a double-bounce return. Under some common assumptions, these  $H/\alpha$  parameters can be related to physical properties of the distributed target.

The second approach, suggested by Freeman and Durden (1998) uses a simple three-component scattering mechanism model, with double-bounce, surface and volume scattering components. Its advantage is in providing directly powers of the canonical scattering mechanisms, suggesting more straightforward interpretation. However, Freeman-Durden decomposition is not rotation-invariant, limiting its applicability. Another problem is overestimation of volume scattering contribution. In order to avoid this problem, in the study we used a modified version of this decomposition, developed in VTT (Antropov et al. 2011).

### **Experimental processing: snow mapping with polarimetric SAR**

Experimental processing included solution of model fitting problem in order to obtain the best agreement between snow maps derived from PolSAR images (shown in Figure 20) and snow maps produced from MODIS data by SYKE. The SAR scene acquired on April 14<sup>th</sup> has already included primarily wet snow, as it can be seen from a rapid increase in the green channel intensity in respective Pauli RGB image. In several previous days temperatures were higher than zero. However, as we are interested in fractional SCA estimation, and the described above algorithm allows discriminating between wet snow and either snow-free (bare-ground) or dry-snow surfaces, three SCA maps were produced for April 25<sup>th</sup>, May 8<sup>th</sup> and May 19<sup>th</sup>, respectively. These were the SAR acquisition days when the ground was neither completely snow covered nor completely snow free.

Results of the threshold ratio fitting with respect to different polarizations for the image acquired on May 8th, during the most active snow melt, are collected in Table 1. An average of images acquired on February 25<sup>th</sup> and March 21<sup>st</sup> is used as a composite dry-snow reference image, while June 1<sup>st</sup> image is used as a bare-ground reference. The RMSE figures (Root Mean-Square Error) appear to be rather good. The obtained results (smaller RMSE) indicate smaller suitability of use of the bare-ground SAR image as a reference when compared to the dry-snow composite image (or any chosen dry-snow scene). A possible explanation is the quite significant bias to overestimation of fractional snow coverage for open bogs and peat land, as these areas exhibited much stronger backscatter for bare ground scene than for dry-snow scenes, with much more significant surface scattering contribution (HH+VV polarization). Optimal threshold values varied quite significantly between different polarizations with the dry-snow reference image, while variation for bare ground was significantly smaller. One can also see that good results (RMSE beyond 0.08) can be obtained with different combinations of polarization channels, taking advantage of different scattering mechanisms exhibited by snow layer depending on snow depth, water content, surface roughness, average grain size etc. The obtained threshold levels are generally in good agreement with wet-dry snow discrimination modeling experiments for RADARSAT-1 C band backscatter (Magagi & Bernier 2003) and experimental fitting for the boreal forest zone (Luoju et al. 2009).

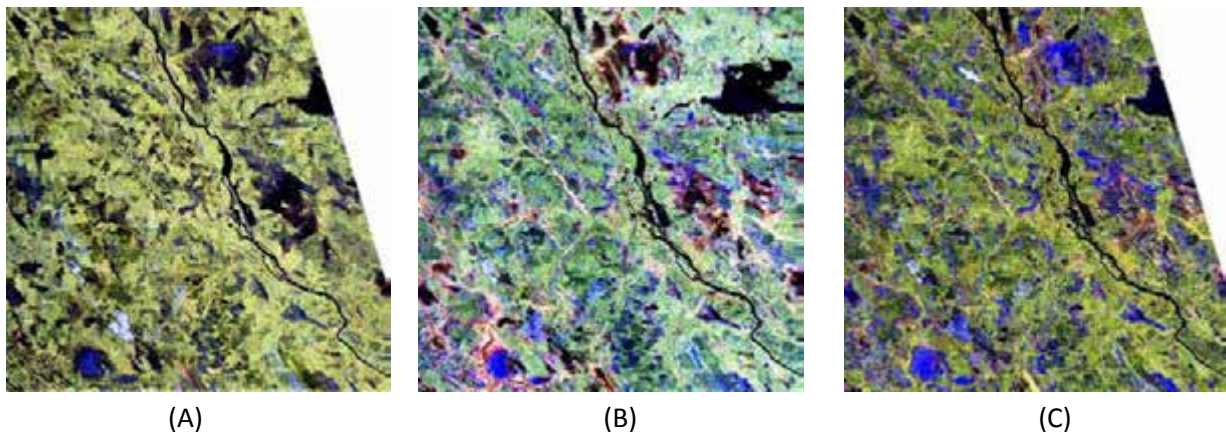


Figure 20. Pauli RGB representations of C band PolSAR data acquired April 24<sup>th</sup> (A), May 8<sup>th</sup> (B), and May 19<sup>th</sup>, 2009 (C). HH-VV is represented by red, HV by green and HH+VV by blue color. © MacDONALD, DETTWILER AND ASSOCIATES LTD., 2009.

Table 1. SCA mapping algorithm parameters for PolSAR image acquired on March 8<sup>th</sup>, 2009.

Processing configuration	Composite dry-snow reference image		Bare-ground reference image	
	Threshold, dB	RMSE	Threshold, dB	RMSE
HH	-0.92	0.0742	-2.15	0.0838
VV	-1.01	0.0767	-2.50	0.0861
HV	0.48	0.0804	-2.16	0.0859
HH + VV	-1.46	0.0782	-2.39	0.0939
Span image	-0.18	0.0762	-2.38	0.0907

The same snow mapping approach was envisaged for production of SCA estimates from PolSAR images acquired on April 25<sup>th</sup> and May 19<sup>th</sup> at 24.6 degree incidence angle. Corresponding dry-snow images (March 8<sup>th</sup> and April 1<sup>st</sup>) were also found to be a better alternative for a reference image than a bare ground image acquired on June 12<sup>th</sup>. However, optimal threshold level estimates for the beginning of snow melting period (April 25<sup>th</sup>) shifted to significantly higher levels, reaching up to 1.9 dB for HH-polarization for April 25<sup>th</sup> image with RMSE of 0.0806. If threshold level was fixed to at least 0 dB for HH polarization, then quite significant underestimation of snow coverage was observed all throughout the scene, with RMSE of 0.2744. On the other hand, for the end of the snow melting season threshold of less than -2 dB proved to be enough to discriminate between wet-snow and bare-ground areas, provided by the May 19<sup>th</sup> scene, when almost all the snow was melted both in open and forested areas.

Snow maps derived from PolSAR are shown in Figure 21. Visual comparison with the land cover/use data did not reveal any significant bias of the produced snow maps towards the presence of forest, when dry-snow images were used as a reference. As snow melting is generally more intensive in open areas than in forested, it gives a good agreement with produced SCA map estimates. However, it is possible that a forest compensation procedure can improve the obtained results, as optimal threshold value for forested and non-forested values differed up to 0.3 dB when processing was organized separately.

The observed high variability of the optimal threshold value strongly limits possibilities of operational snow cover mapping. One possible way to overcome this obstacle is additional calibration of the change-detection model using some additional external data. It can be e.g. coarse resolution data from a passive microwave space-borne sensor, or some ground reference data. In this study we use snow data collected in a 4 km long rectangular track to obtain reference SCA samples at different resolution levels: 100 m x 100 m, 500 m x 500 m and 2 km x 2 km. The idea behind this approach is that relating a reference SCA to SAR backscatter can provide an optimal threshold value, to be further supplied to a snow mapping algorithm. Obtained optimal values deviated from those given in Table 5.2.1 by 0.3–1.1 dB when using dry-snow composite image, resulting in RMSE exceeding 0.082, with accuracy still being higher than provided by use of bare-ground reference imagery. Keeping in mind that a MODIS SCA estimate is not error free ground truth data, this discrepancy seems to be acceptable. Altogether it indicates a high potential of the suggested approach, if more samples for a threshold calibration are measured.

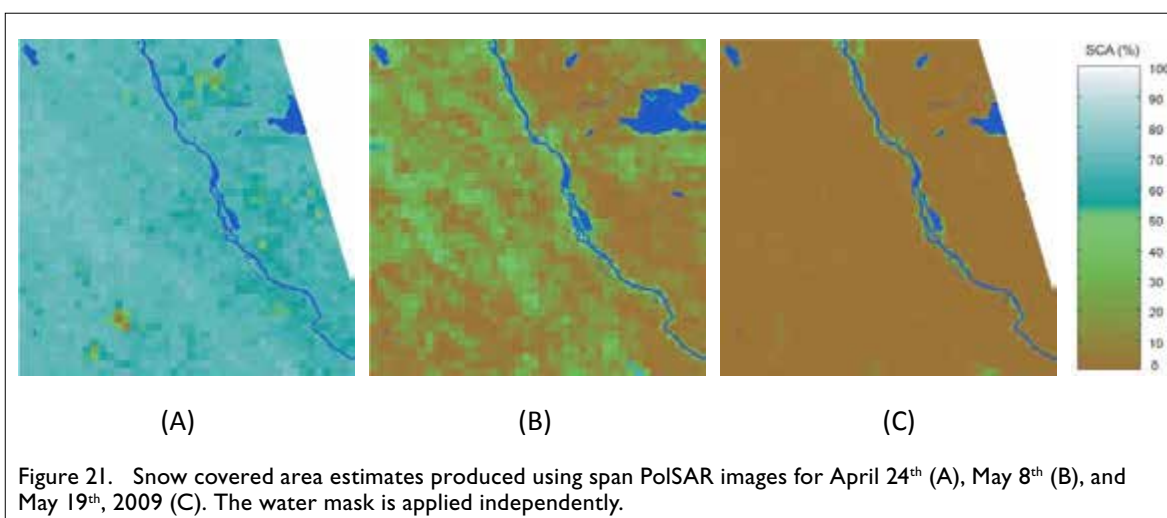


Figure 21. Snow covered area estimates produced using span PolSAR images for April 24<sup>th</sup> (A), May 8<sup>th</sup> (B), and May 19<sup>th</sup>, 2009 (C). The water mask is applied independently.

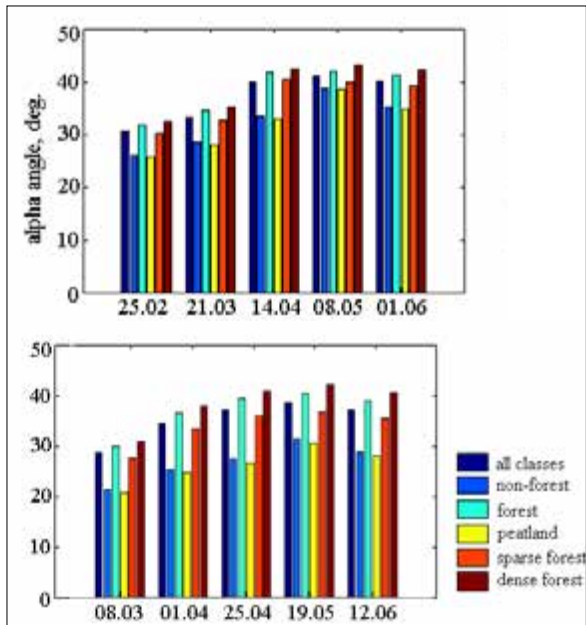
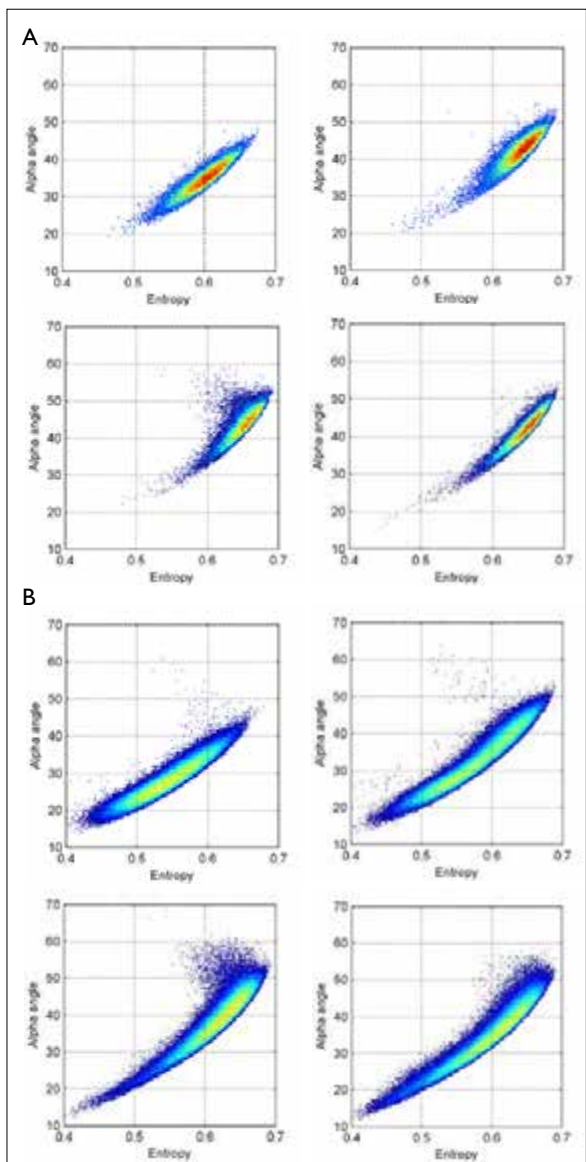


Figure 22. The temporal dynamics of alpha angle during snow melting season for different land cover/use classes: (left) incidence angle 38.4 degrees, (right) incidence angle 24.6 degrees.



## Dynamics of polarimetric observables during snow aggregation and melting season

When analyzing results provided by the Cloude-Pottier decomposition approach, the general dynamics is described by a slow growth in volume scattering contribution during the snow aggregation period, followed by a much stronger growth during the snow melt itself and further less significant decrease in summer scenes. This dynamics is clearly followed for all the land cover classes (Figure 22), indicating a quite good penetration through forest canopy at C band, especially under frozen conditions. As expected, the contrast between different land cover classes is significantly higher at higher incidence, with surface scattering being dominant for open areas and volume scattering for forested areas. During the start of the snow melt (April 14<sup>th</sup>, Figure 22) a more significant growth in volume scattering for forested areas can be explained not only by the increased backscatter from wet snow, but also by forest transition to non-frozen state. As the snow melting process becomes more active, non-forested areas demonstrate quick growth in volume backscatter (May 8<sup>th</sup>, Figure 22), while for forested areas change in overall backscatter due to wet snow change contribution is much less significant. At the end of the monitoring period, once there is no snow cover, both forested and non-forested areas show decline in volume scattering, though rather small for forested areas but quite strong for open areas.

These observations indicate potential for use of the alpha angle feature in snow mapping with respect to different land cover classes. They also support our previous conclusions on higher suitability of dry-snow scenes over snow-free (bare ground) scenes for use in change detection based snow mapping, as contrast between dry snow and wet snow scenes appears to be much higher than between wet snow and snow free terrain, especially over forest covered region. It also reveals a potential of using a volume scattering backscatter component (or alpha angle) alone for snow mapping. Further analysis performed in alpha/entropy plane for selected land cover/use classes is shown in Figure 23, being in line with the discussion above and additionally indicating significant growth in entropy during the most active phase of snow melt on May 8<sup>th</sup>.

Figure 23. Temporal dynamics of selected land cover classes' characteristics in alpha/entropy plane during snow melting season for different land cover/use classes: (A) dense coniferous forest over peat land, (B) open bogs. Columns: 1 - March 21<sup>st</sup>; 2 - April 14<sup>th</sup>; 3 - May 8<sup>th</sup>; 4 - June 1<sup>st</sup>, 2009.

Figure 24 shows results of application of the modified 3-component Freeman-Durden decomposition to the analysis of PolSAR data acquired on April 14<sup>th</sup> (Figure 24A, B) and May 8<sup>th</sup> (Figure 24 C, D). Two different visualization schemes were used. Imagery in Figure 24 A, C show logarithm of powers of scattering mechanisms with further contrast stretching, while for representation in Figure 24 B, D no logarithmic operation was performed. The relative double bounce, surface and volume contributions are depicted as red, blue and green components of the color-composite images. The latter approach allows to clearly identify dominating scattering mechanism and is easy to use in rule-based approaches. In particular, an area where double bounce contribution becomes dominating for May 8<sup>th</sup> seems to clearly indicate a flooding event extent. This opens possibilities for the near real-time identification and monitoring of such potentially hazardous events as flooding from PolSAR data.

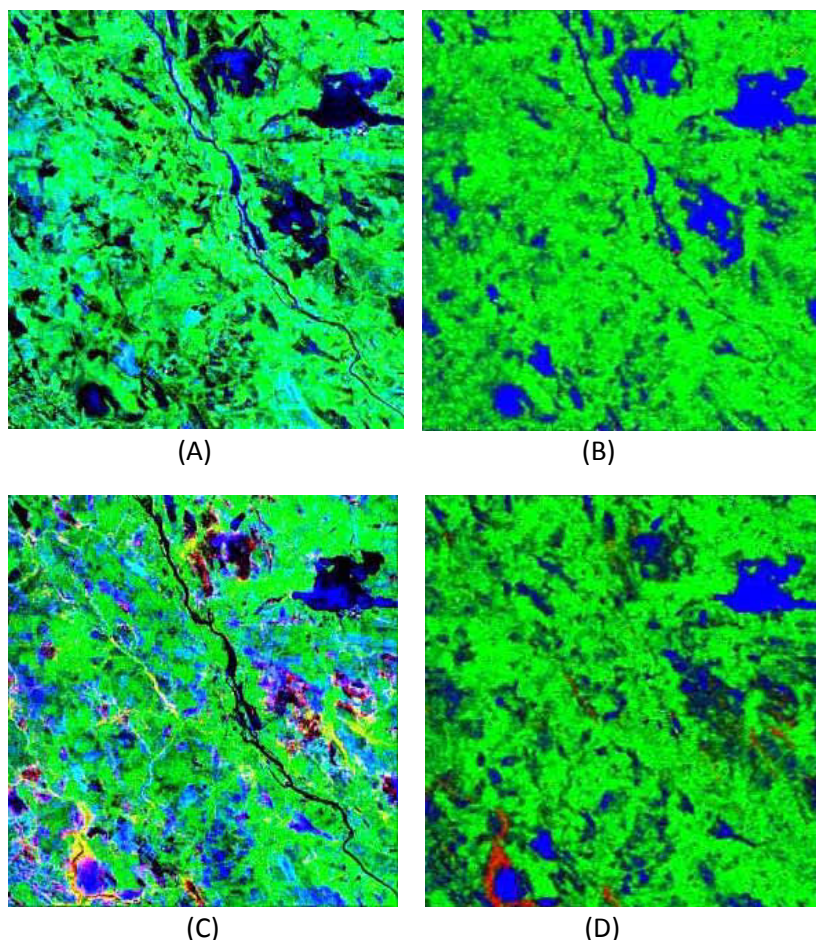


Figure 24. Towards flooding event detection: different representations of the modified 3-component decomposition, red – double bounce, blue – surface, green – volume scattering mechanism powers; (A),(B) – April 14<sup>th</sup> ; (C),(D) – May 8<sup>th</sup>, 2009; (A),(C) – powers in dB with contrast stretching; (B),(D) – relative contributions of scattering mechanisms to the total power.

## Conclusion

Different modifications of the single-reference-image snow cover mapping method were implemented and analyzed for multi-polarization data, with several combinations of polarimetric observables as well as total backscattered power used in the study. The optimal threshold level and its influence on the snow mapping accuracy, as well as a rational strategy for choice of an optimal reference image were investigated.

Practically all the combinations appeared to be fruitful under some adaptations, revealing backscatter response due to different phenomena of electromagnetic wave interaction with snow cover at the snow-ground and air-snow interfaces, as well as within the snowpack. The best results were obtained using horizontally polarized channel and total power image (span of the covariance matrix), exhibiting generally good correlation with snow maps produced from MODIS optical data. High variability of optimal threshold ratio for discriminating between wet snow and bare ground was observed from scene to scene in multi-temporal and multi-polarization aspect. It suggests that no optimal threshold value can be fixed to process all the given scenes simultaneously, leading to necessity of some kind of external calibration of the snow mapping change-detection model. The snow covered area maps, as well as the original PolSAR imagery, can be supplied for demonstration purposes to the demonstration system (Section 3).

Strong changes in the temporal dynamics of selected polarimetric features were identified for several classes of the land cover data. They proved to provide a

clear indication of the snow melting and flooding events in the area, for instance a significant increase of the volume scattering from wet snow, and a rapid increase of the double-bounce scattering mechanism contribution in backscatter from flooded forest. It reveals a potential of future use of polarimetric features as event indicators in environment monitoring applications.

### 5.3

## Freeze/thaw state of the soil

*Tuomo Smolander, Kimmo Rautiainen, Juha Lemmetyinen*

One aspect investigated within *FloodFore* was the availability or generation of a soil freeze/thaw state product from EO data, which could be integrated into the multi-source hydrological forecasting system. No specific sensors exist which are dedicated to the monitoring of the soil freezing state; several EO missions provide data on the low frequencies (L- to C and X bands) which can be applied for this purpose. These frequencies are sensitive to the changes of dielectricity that the soil freezing process causes, and have a sufficient penetration depth into the soil to provide meaningful observations below the immediate soil surface. A two-fold approach was chosen for the investigation

- Generation of large-area, coarse scale freeze/thaw state indicators from recently available passive microwave sensors (e.g. SMOS)
- Investigation of the applicability of SAR imagery in a change-detection algorithm to provide information on spatial variations of the soil freezing state at a high spatial resolution

### Soil frost detection from active microwave observations

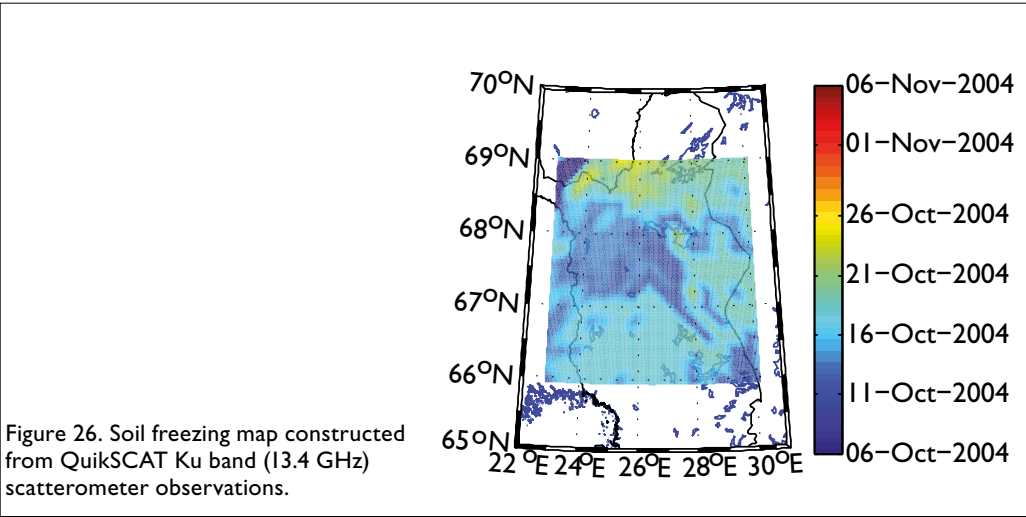
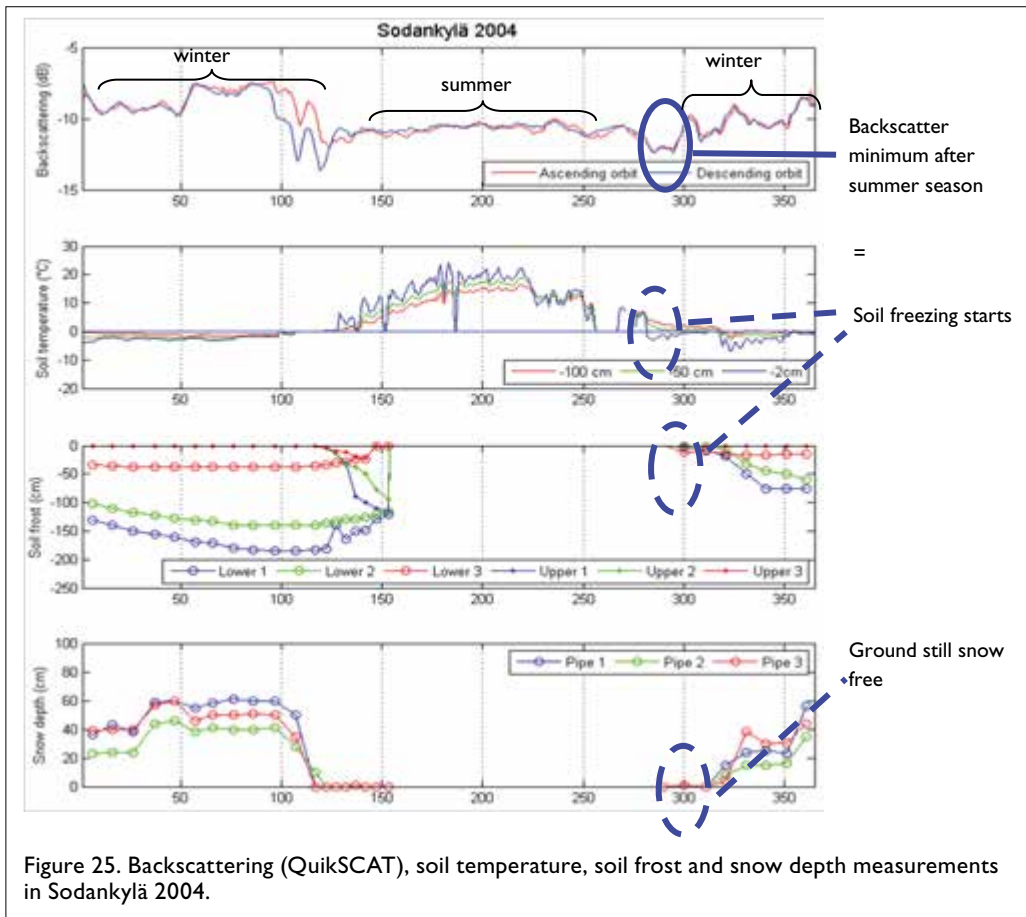
The feasibility of determining soil freezing using active microwave instrument was investigated. As a first step, backscatter observations from the QuikSCAT satellite radar (Ku band, 13.4 GHz) were applied. The QuikSCAT mission was terminated in autumn 2009 due to instrument failure; however, historical datasets are available. QuikSCAT was not a SAR instrument but a scanning scatterometer device; thus the spatial resolution is limited. The instrument, however, provided global coverage and as such provides a useful tool for coarse-scale investigations.

A change detection algorithm was employed to detect the moment of soil freezing in the autumn. The detected backscattering coefficient decreases as the soil freezes due to the change in dielectricity of the soil, causing a clear contrast to observations earlier in the autumn. However, at Ku band, snow cover gradually will increase the backscatter signal through volume scattering, eventually masking the ground signal.

In a first test, the date of the minimum backscatter during autumn was used to mark the onset of soil freezing (Figure 25). The results were compared to in situ weather station and soil frost measurements and showed the method to be feasible even though the resolution and noise levels of the instrument were not optimal.

The method was applied for a range of QuikSCAT observations over Northern Finland; the resulting map of soil freezing for the autumn of 2004 is depicted in Figure 26.





As the investigation using low-resolution QuikSCAT data was encouraging, preliminary investigations for applying a similar method using high-resolution SAR at a lower frequency band (C band) were carried out. C band would have the advantage of higher penetration depth, and relative insensitivity to snow cover. For the investigation, a dataset of ESA EnviSAT/ASAR images at 1 km resolution were acquired. Figure 27 demonstrates an exemplary image pair from autumn 2010 over the Sodankylä region. The first image is from Oct 5, 2010, when the soil surface was completely thawed according to in situ data. The latter image is from directly after soil freeze onset. The overall backscatter in the latter image can be seen to be clearly decreased, from an average of  $-6$  dB on Oct 5<sup>th</sup> to  $-9.5$  dB on Oct 17<sup>th</sup>.

The 1 km resolution does not allow very clear separation of land cover features directly from the images; however, areas with distinct land cover types can be singled out. Figure 27 shows the measured backscatter coefficient over a  $3 \times 3$  km forested area close to Sodankylä (indicated in Figure 27). The drop in backscatter indicates a clear change on October 17<sup>th</sup>. This corresponds to the first measured sub-zero temperatures in the Sodankylä region (Figure 29).

Future investigations will continue the application of high resolution C band imagery, which from EnviSAT/ASAR is available up to 30 m resolution.

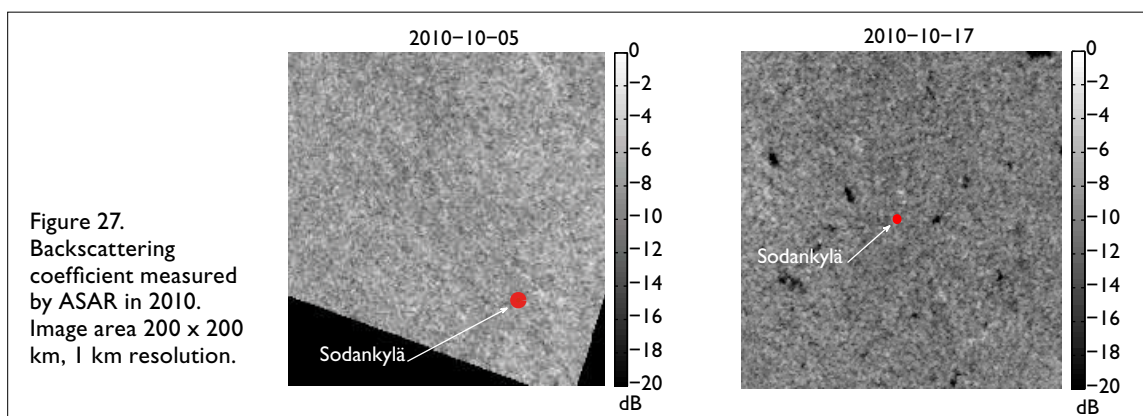


Figure 27. Backscattering coefficient measured by ASAR in 2010. Image area  $200 \times 200$  km, 1 km resolution.

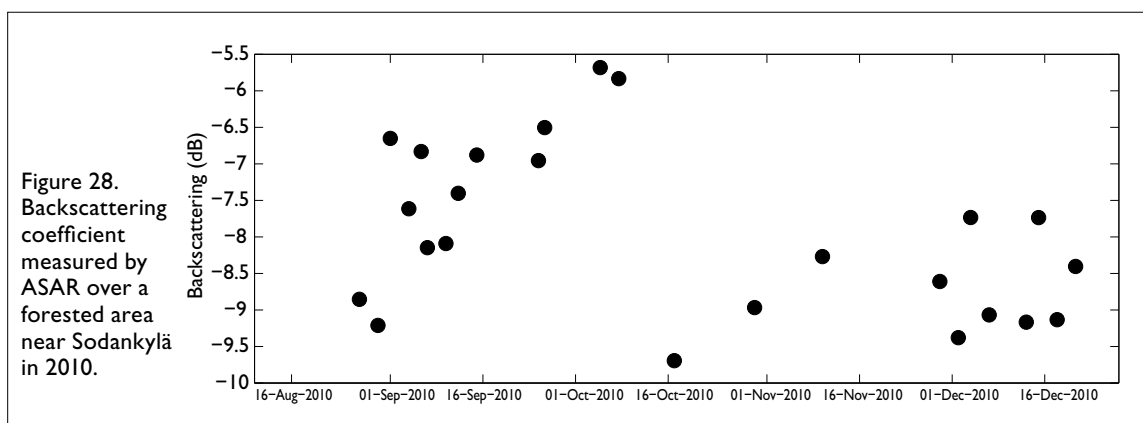


Figure 28. Backscattering coefficient measured by ASAR over a forested area near Sodankylä in 2010.

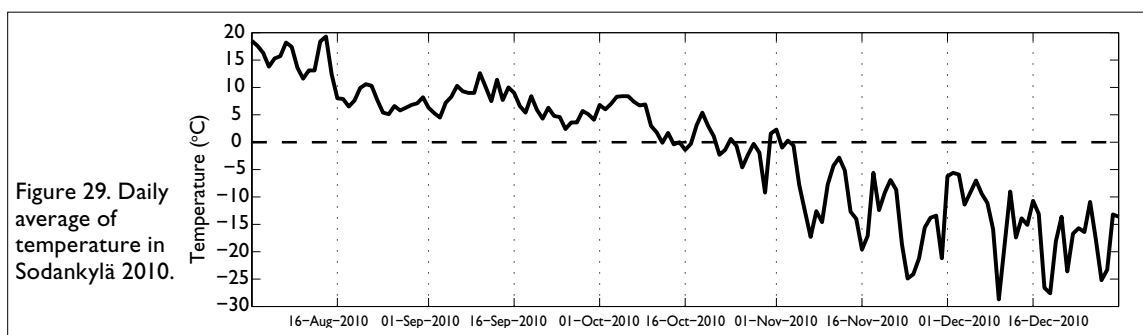


Figure 29. Daily average of temperature in Sodankylä 2010.

## Soil frost detection from passive microwave observations

Possibilities for soil-freeze/thaw state detection from passive sensors were increased with the launch of ESA SMOS (Soil Moisture and Ocean Salinity) mission in 2009. The satellite payload measures the brightness temperature at L band with the novel concept of interferometric radiometry, providing images of the area observed.

Related to the SMOS mission, FMI operates a calibration/validation instrument for SMOS, the ELBARA-II dual-polarization L band radiometer. The instrument is situated at the FMI-ARC station in Sodankylä, Finland. Within the framework of the *FloodFore* project, ELBARA-II measurements were used in development of a soil frost detection algorithm (Rautiainen et al. 2011). Figure 30 shows the time series of Elbara-II observations against available in situ data on snow cover and soil frost depth at the site. The algorithm has been applied SMOS observations resulting to the first preliminary soil freeze/thaw maps for Northern Finland.

### Algorithm development

Two noticeable characteristics can be drawn from the annual behaviour of ELBARA-II L band observations: (1) There is a clear increase in brightness temperature from the summer average to winter average. This is more evident at higher incidence angles and at H-polarization. (2) The brightness temperature polarization difference (Vertical-Horizontal polarization) is much smaller during winter compared to the summer average. Based on above mentioned two characteristics, the soil freeze/thaw state can be determined from L band observations using a simple change detection algorithm. It should be noted that L band measurements are largely insensitive to snow cover.

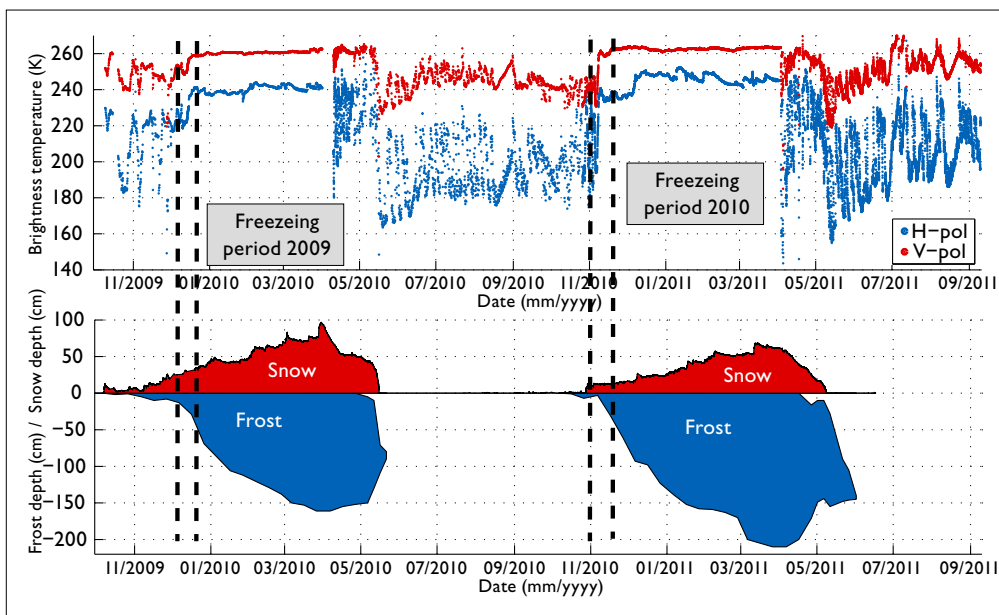


Figure 30. ELBARA-II measurement at 50 degrees incidence angle and soil frost / snow depth information gathered from in-situ measurements (frost tubes and acoustic snow depth instrument). Autumn: Rapid increase in soil freezing is seen as an increase in ELBARA-II brightness temperature.

The so-called frost factor (FF), describing the change in both H-polarization and the H/V-polarization brightness temperature (Tb) relation, is shown in Figure 31 for Elbara-II observations at the FMI-ARC station. The developed change detection algorithm is based on changes in the Frost Factor after the summer period, and defining the target as frozen as a certain threshold in the change of the FF has been surpassed. By using Elbara-II observations and in situ data, a threshold value of 75 % change in FF compared to the summer period was determined to match *in situ* observations of soil freezing, and was used as a starting point in the algorithm.

### SMOS data for regional frost detection at coarse resolution

A next step in testing the newly developed change detection algorithm was to apply it for the SMOS reprocessed first year data over a selected area in Northern Finland (see Figure 32). Due to the nature of the sensor, SMOS data is of fairly coarse resolution. The brightness temperatures used has been resampled to a resolution of approx. 40 x 40 km which corresponds to the instruments true resolution.

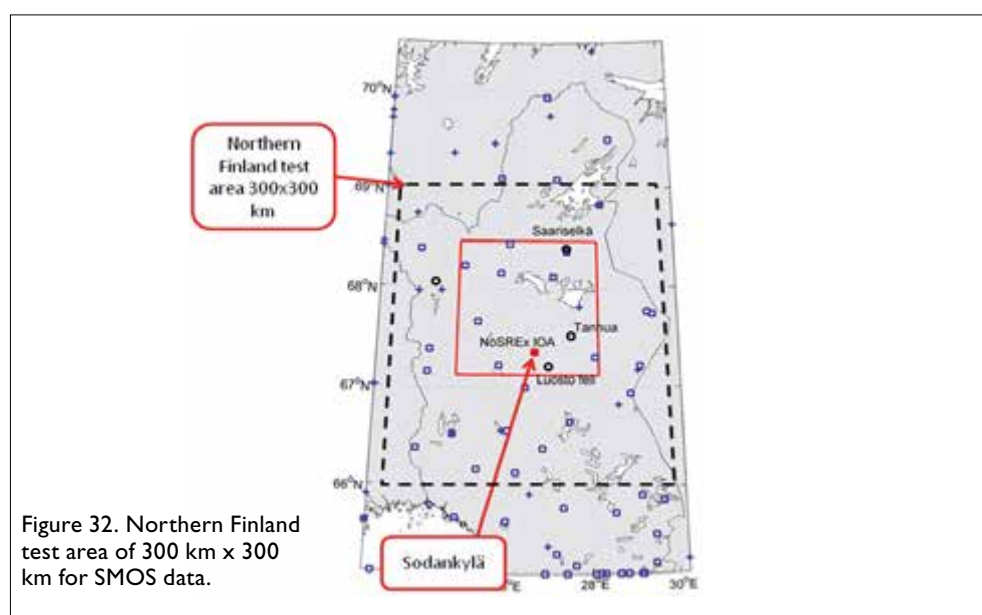
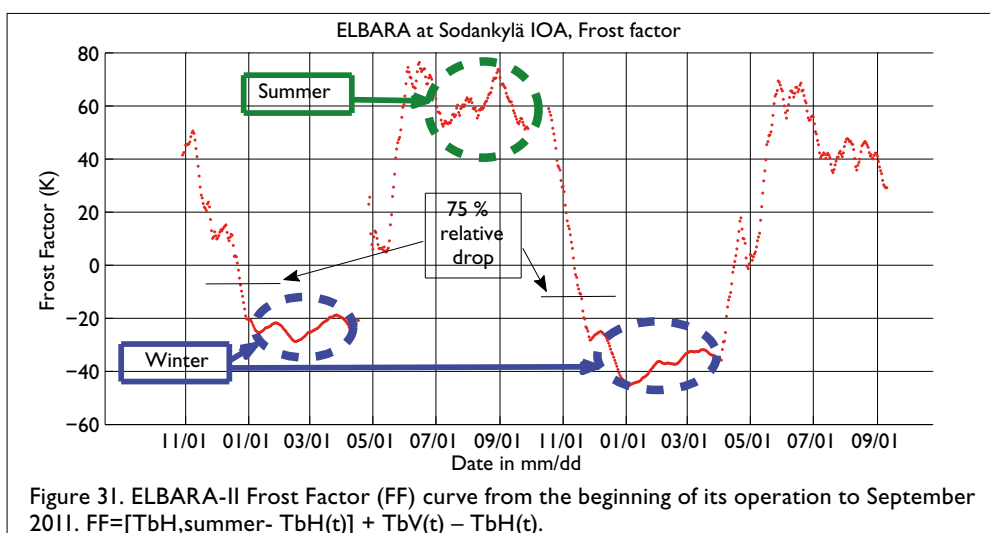


Figure 33 shows the frost factor curve for SMOS data for one grid cell, corresponding to the location of the FMI-ARC station (and the Elbara-II radiometer) in the autumn of 2010. The evolution of the FF from SMOS data shows very similar features with the corresponding curve of ELBARA-II. The dynamic range is smaller, but the freezing period is clearly noticed as a continuous, fairly rapid decrease in the FF value. Using the change detection algorithm for every individual SMOS grid cell, the moment of soil freezing was determined, thus obtaining a “soil freezing date” for each cell. A resulting map of soil freezing dates for Northern Finland in the autumn of 2010 is shown in Figure 34. The date given in the map represents the situation of firmly frozen soil (depth of 20-30 cm). The detected soil freezing dates span a period of approx 35 days.

Results for freezing date based on SMOS data were tested against in situ data on the soil state. The locations of in situ observations are indicated in Figure 32; the data consists of manual measurements of soil freeze/thaw over several land cover types. The results of the comparison are illustrated in Figure 35. For each station, three different tube observations are given for bog, open area and forest sites, from top to bottom. Colour code indicates the time line when frost depth evolved from 0 to 10 cm, 10 to 20 cm, 20 to 30 cm and 30 to 40 cm. The triangle is the date for the soil frost state obtained from SMOS (75 % change in FF criterion). A preliminary comparison is in fairly good coherence with the in situ data, but further investigation is needed before the algorithm can be applied in an operative sense.

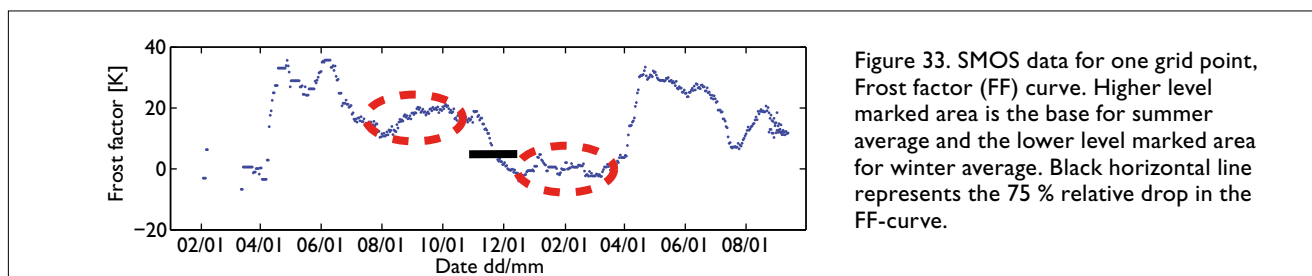


Figure 33. SMOS data for one grid point, Frost factor (FF) curve. Higher level marked area is the base for summer average and the lower level marked area for winter average. Black horizontal line represents the 75 % relative drop in the FF-curve.

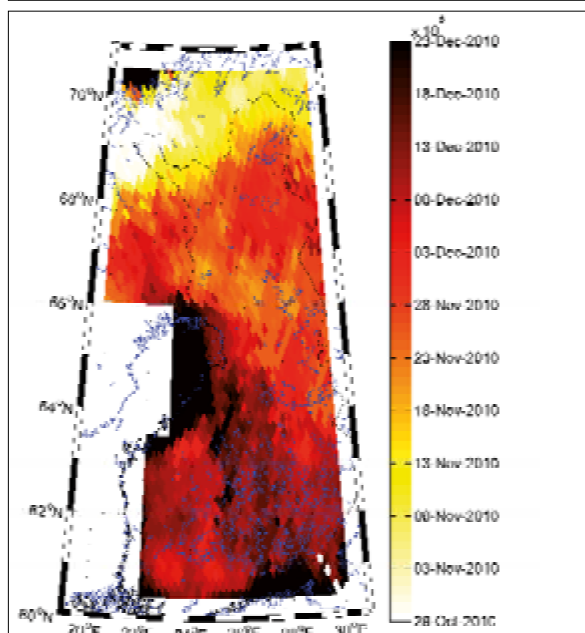


Figure 34. Soil freezing map constructed from SMOS Level 1 C data using the FF-curves and change detection algorithm. The colour code indicates the moment (or date) when the soil at that area is considered to be firmly frozen by the algorithm. The circled asterisks are the frost tube locations.

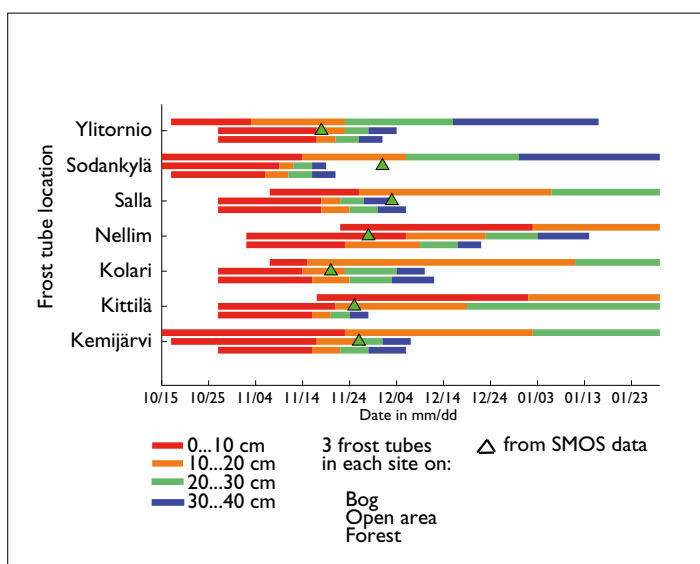


Figure 35. Comparison of frost tube observations and freezing date estimated from SMOS data using FF-curve and change detection algorithm.

## Improving passive microwave estimates through inclusion of lake ice characteristics

Juha Lemmetyinen

The retrieval approach used in the *FloodFore* SWE product is susceptible to inaccuracies related to mixed pixel effects caused by the relatively coarse resolution of passive microwave instruments. One of the potential sources of error arises from the differing background emission from water surfaces, such as lakes and rivers, compared to that of the surrounding landscape. The presence of lakes may cause a bias in any SWE estimate based on passive microwave data. A possible way to mitigate for this error is the inclusion of lakes and lake ice in the forward model used for retrieval.

An investigation to this effect was made for three winter periods, covering the years 2005–2008. In order to demonstrate the effect of lake ice on observations, two scenarios were considered: (1) the influence of lakes was excluded and (2) included in the forward model. For (2), the current forward model required to be updated for simulation of multiple-layer snow/ice structures (Lemmetyinen et al. 2010). The model was validated against experimental airborne data over lake ice in Canada (Gunn et al. 2011). The full investigation is detailed in Lemmetyinen et al. (2011).

The lake ice conditions for the retrieval were set from available in situ information; the data consists of ice depth measurements performed operationally by the Finnish Environment Institute (SYKE). Over 50 lakes are surveyed regularly for ice depth, snow on ice depth and ice stratigraphy. Snow course measurements by SYKE were applied as reference for the retrieved SWE estimates. Data from over 120 snow courses around the country were available for the investigation.

Figure 36 demonstrates an example of gridded SWE estimate maps obtained for one day (January 1<sup>st</sup>, 2006), when (a) ignoring the effect of lakes in the forward simulation module and (b) compensating for lake influence in the forward simulation. Also shown is the difference of the retrieved SWE value. It can be seen that including lakes in the forward model generally raises SWE estimates for the southern Finland lake district, and over single large lakes in northern parts of the country. The difference in measured SWE is up to 50 mm in some individual grid cells with significant lake fraction.

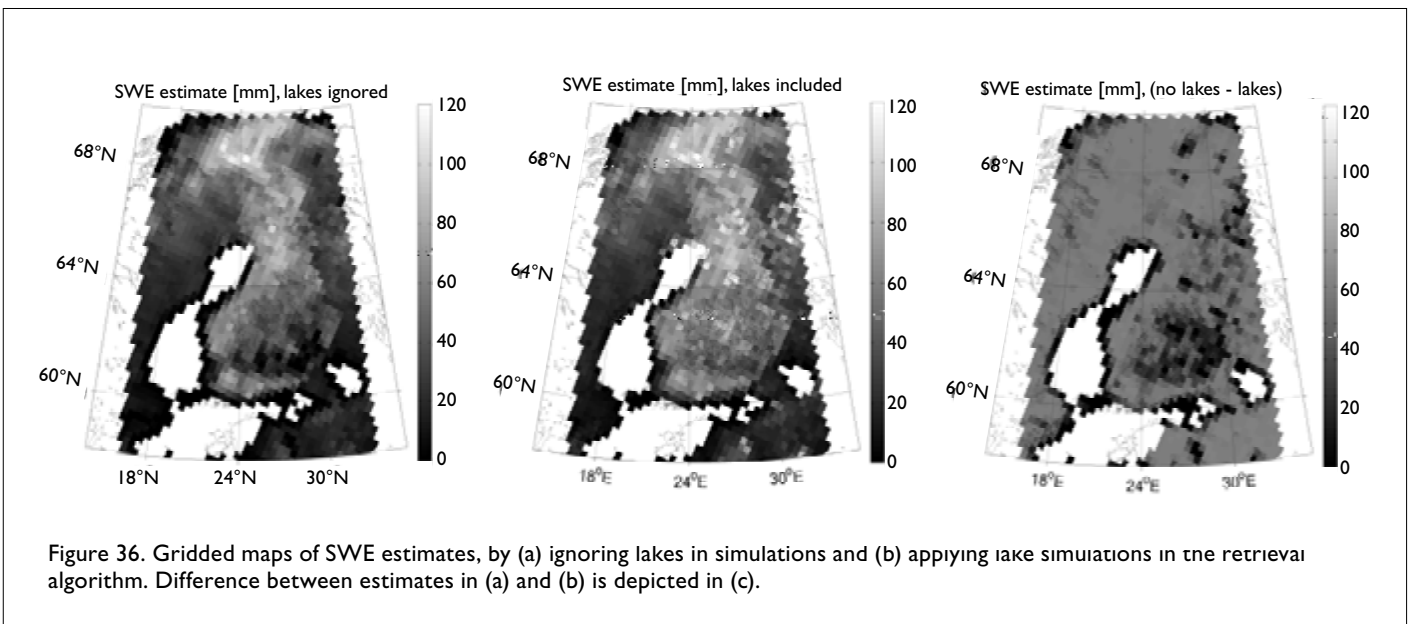
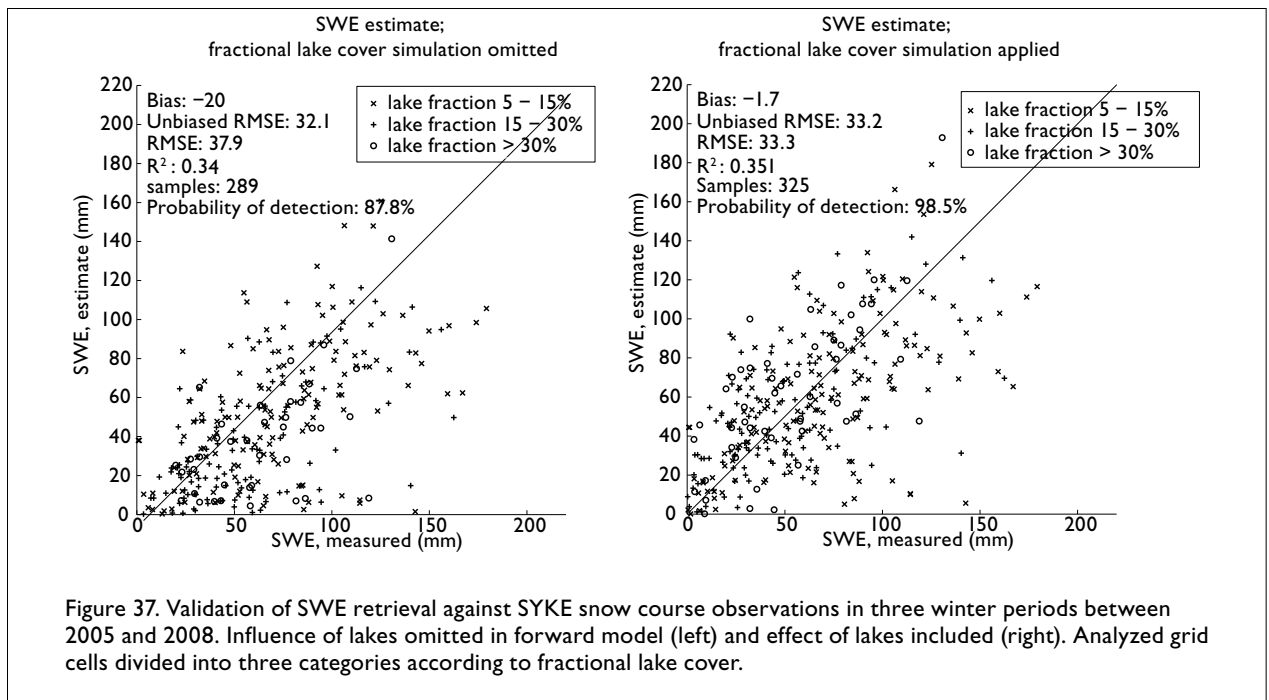


Figure 36. Gridded maps of SWE estimates, by (a) ignoring lakes in simulations and (b) applying lake simulations in the retrieval algorithm. Difference between estimates in (a) and (b) is depicted in (c).

Validation of the SWE results for a dataset spanning three winter periods was conducted against SYKE snow course measurements; Results from both scenarios (lakes/no lakes), are shown in Figure 37 for regions with above 5 % fractional lake cover. The inclusion of lake ice simulations can be seen to improve estimate accuracy; the overall bias error is reduced from -20 to -1.7 mm and the RMS error from 38 to 33 mm.

The presented method indicates a possible way to improve the current FloodFore SWE product. The improvement is significant for areas with high density of lakes and other water surfaces. However, the main hindrance of the presented method is the requirement of *in situ* information on lake ice. For the area of Finland, such data is currently available, but regarding wider applicability of the method similar data is scarce for other regions in the Northern Hemisphere. A future possibility is to apply a physical model for predicting the prevailing lake ice conditions (ice onset, ice thickness, snow depth on lake ice).



## 6 Commercialisation planning

*Jukka Kiviniemi*

### Background

The targets of a commercialization planning are to identify commercialization scenarios for FloodFore results, and to define next steps for commercialization (at least one scenario). The plan was disseminated in FloodFore steering group meeting at May, 2011. In this report, main findings of this commercialization plan are presented together with proposed next research steps to support the commercialization.

The original commercialization setting is presented in Figure 38. The focus of commercialization is how to implement the system or part of it for other regions of the world.

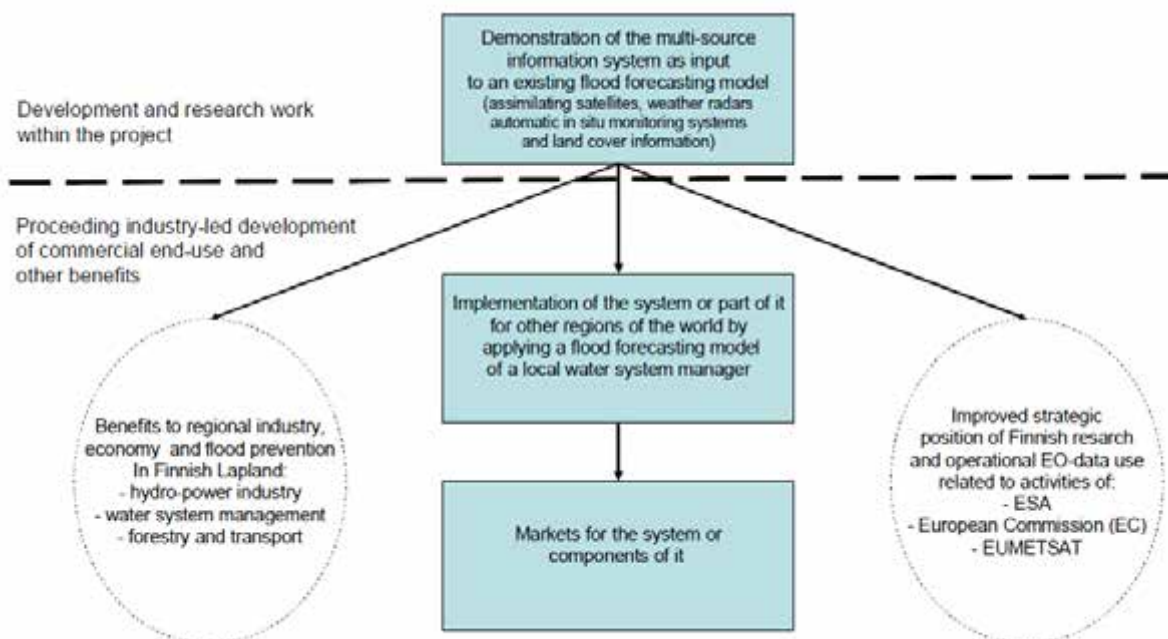


Figure 38. The original commercialisation setting.



## Methodology and value chain

The methodology of commercial planning consists of several major tasks: literature studies to evaluate overall situation of the market, interviews with FloodFore project participants to examine usability of the results and additional value caused by applying the results. Furthermore, discussions have been performed with commercial entities about productizing the FloodFore results and composing the feasible business model.

An important factor in the business model is in which part of value chain the results of FloodFore are applicable, Figure 39 presents a simple value chain in environmental data collection and monitoring. The freedom of information boundary, enforce at least by EU directives and US government, defines which part of data should be publicly available. This boundary is somehow fuzzy and there are differences between legislations, so a careful analysis should be performed when designing global business models in this arena.

## Results

In the business model analysis, we identified three major commercialization scenarios:

1. SWE/SCA analysis for hydropower companies. In this scenario, a service is offered for hydropower companies to compute snow situation and energy value of the snow in the hydrological area of the hydropower company. This scenario enables a global service concept. The main restriction for a global service concept is that a plug-in to local hydrological model is required in every area where the service is applied.
2. Enhancing hydrological models with SWE/SCA measurements. In this scenario, reliable SWE/SCA computation methods are licensed to national weather and hydrological institutes, or to consulting organization, i.e. DHI. According to FloodFore results, hydrological models can be significantly enhanced with proposed methods, especially in abnormal weather situations. The main challenge here is interpretation of freedom-of-information boundary and how the additional value caused by more reliable measurement can be monetized.
3. SWE/SCA presentation mashups for tourist info, flood situation reports and warnings, and similar kind of solutions. In this scenario, SWE/SCA computation methods are licensed to weather service companies, i.e. Foreca to provide additional services.

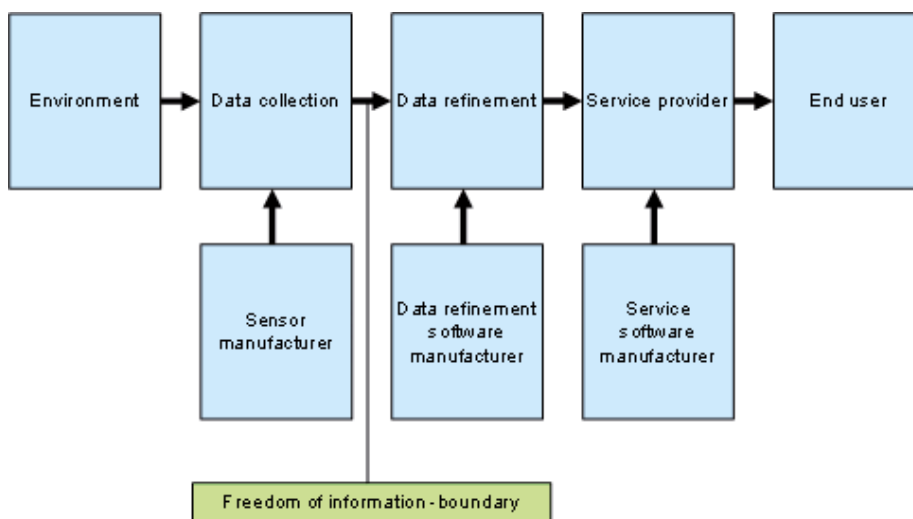


Figure 39. A simple value chain in environmental data collection and monitoring.

## Open issues and next steps

From these scenarios, scenario 1 was selected for further analysis. The main open issues related to commercializing scenario are identified to be:

- Analysis of feasibility and interoperability of other hydrological models to use SWE information
- Cost of data to compute SWE/SCA (satellite images, etc.)
- Proving real value of the SWE/SCA calculation in real environment other than Finland

These steps have been partially performed in the FloodFore project. We propose following next steps to be performed in subsequent projects to support commercialization activities with research:

- Practical demonstration in another location and with another hydrological model
- Analysis of robustness and accuracy of the model with SWE information in general setting
- Composing business case based on learnings from demonstrator to quantify additional value

One practical idea is to include commercialization actions above to the MMEA project as a part of value chain presented in Figure 40. The proposed SWE/SCA measurements can be modeled as a service in this framework. Furthermore, there are a lot of relevant commercialization partners in MMEA project which can utilize the results from the FloodFore project.

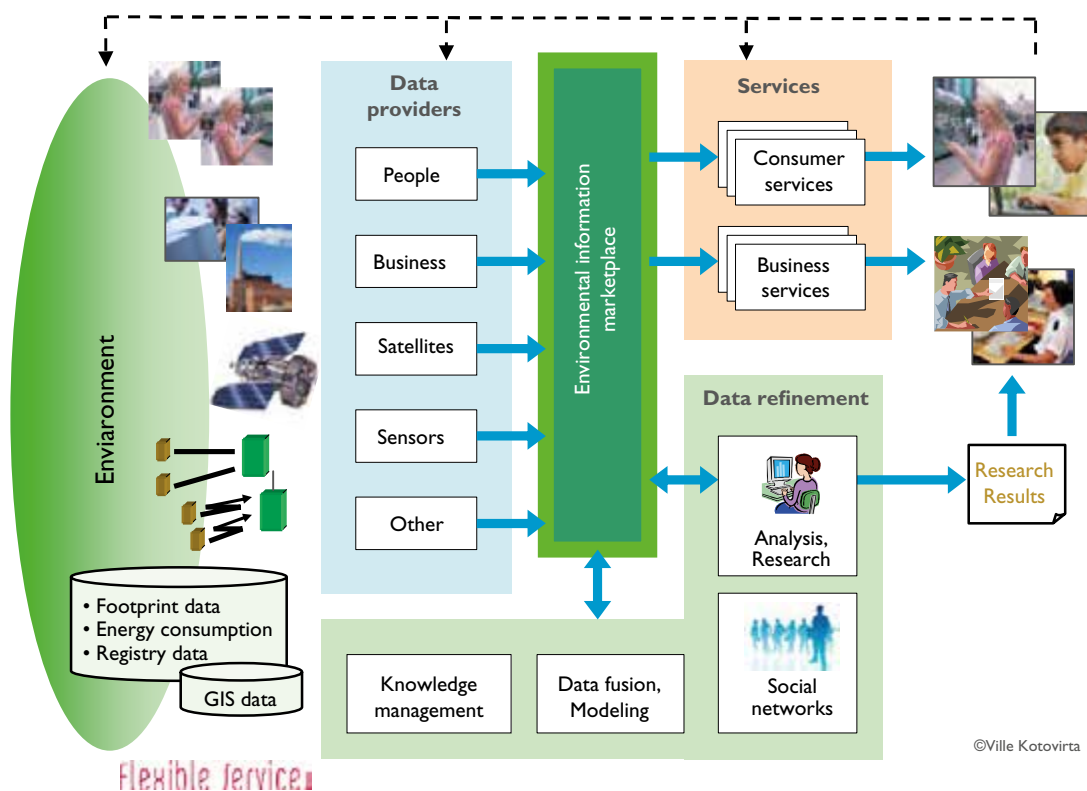


Figure 40. Value chain of the environmental information (MMEA project).

## 7 Conclusions

The FloodFore project focused on the development and implementation of new methodologies and approaches to map hydrological variables, important for the water cycle at northern latitudes, from the combined remote sensing and *in situ* observational data. The objective was also concerned with the demonstration of multi-source information systems as well as the use of new products as input to hydrological forecasting systems. The key achievements include:

- Implementation and validation of the satellite data-aided snow (SWE) mapping system for the region of Finland. The technique has been implemented for the operational use at SYKE to provide information on the amount of snow. This information is currently operationally assimilated to hydrological forecasting system (WSFS). The performed analysis indicates that satellite data-based SWE information is beneficial to operational hydrological forecasting purposes.
- Implementation of the novel weather radar-based approach to map cumulative precipitation with the aid of calibration data from discrete rain gauges. The methodology is able to provide quantitative estimates e.g. on the diurnal total precipitation, which has not been possible before for the weather radar system of Finland (currently restricting to non-winter conditions as rain gauge network in case of Finland does not provide reliable data for the solid precipitation).
- Demonstration of new satellite data-based techniques for the mapping of soil freezing in forests and bogs.
- Development and demonstration of synergistic data fusion systems in the mapping of SWE with a high resolution from the combined space-borne data sets including passive microwave (spatial resolution 25 km) and radar (spatial resolution ~100 m) observations.
- Demonstration of multi-source information system for the visualization and analysis of spatially distributed multi-temporal observation/monitoring data (relevant e.g. to situation awareness system development). The demonstration system was implemented to include data products on (a) weather radar-derived cumulative precipitation, (b) passive microwave satellite-derived SWE (c) optical satellite data-based fractional snow coverage data products and (d) WSFS hydrological model forecasts.

The developed new techniques are already in use improving the quality and performance of SYKE's and FMI's operational systems and services. They may lead to new commercial applications as well (in the field of hydrological monitoring/forecasting). The investigated methodologies have also practical potential for forestry (timber collection) in case of products related to soil freezing and thawing (snow melt).

## REFERENCES

- Aaltonen, J., Hohti, H., Jylhä, K., Karvonen, T., Kilpeläinen, T., Koistinen, J., Kotro, J., Kuitunen, T., Ollila, M., Parvio, A., Pulkkinen, S., Silander, J., Tiihonen, T., Tuomenvirta, H. and Vajda, A. 2008. Rankkasateet ja taajamatulvat (RATU). Suomen ympäristö 31/2008, 36–48. (<http://www.ymparisto.fi/default.asp?contentid=304648&lan=fi&clan=fi>)
- Antropov, O., Rauste, Y. and Häme, T. 2011. Volume scattering modelling in PolSAR decompositions: Study of ALOS PALSAR data over boreal forest. *IEEE Transactions on Geoscience and Remote Sensing*, 49(10), 3838–3848.
- Cloude, S. R. and Pottier, E. 1997. An entropy based classification scheme for land applications of polarimetric SAR. *IEEE Transactions on Geoscience and Remote Sensing*, 35(1), 68–78.
- Freeman, A. and Durden, S. L. 1998. A three-component scattering model for polarimetric SAR data. *IEEE Transactions on Geoscience and Remote Sensing*, 36(3), 963–973.
- Gunn, G. E., Duguay, C. R., Derksen, C., Lemmetyinen, J. and Toose, P. 2011. Evaluation of the HUT modified snow emission model over lake ice using airborne passive microwave measurements. *Remote Sensing of Environment*, 115(1), 233–244.
- Härmä, P., Teiniranta, R., Törmä, M., Repo, R., Järvenpää, E. and Kallio, M. 2004. Production of CORINE2000 land cover data using calibrated LANDSAT 7 ETM satellite image mosaics and digital maps in Finland. In: *Proc. International Geoscience and Remote Sensing Symposium*, 4, 2703–2706.
- Koistinen, J., Pohjola, H. and Hohti, H. 2003. Vertical Reflectivity Profile Classification and Correction in Radar Composites in Finland. In: *31th International Conference on Radar Meteorology*, American Meteorological Society, Seattle, Washington.
- Koskinen, J., Pulliainen, J. and Hallikainen, M. 1997. The use of ERS-1 SAR data in snow melt monitoring. *IEEE Transactions on Geoscience and Remote Sensing*, 35(3), 601–610.
- Kärnä, J.-P., Pulliainen, J., Lemmetyinen, J., Hallikainen, M., Lahtinen, P. and Takala, M. 2007. Operational Snow Map Production for whole Eurasia using Microwave Radiometer and Ground-based Observations. In: *Proc. IEEE 2007 International Geoscience and Remote Sensing Symposium (IGARSS'07)*, Barcelona, Spain, July 23–28, 1456–1459.
- Lemmetyinen, J., Pulliainen, J., Rees, A., Kontu, A., Qiu, Y. and Derksen, C. 2010. Multiple Layer Adaptation of HUT Snow Emission Model: Comparison with Experimental Data. *IEEE Transactions on Geoscience and Remote Sensing*, 48(4), 2781–2794.
- Lemmetyinen, J., Kontu, A., Kärnä, J.-P., Vehviläinen, J., Takala, M. and Pulliainen, J. 2011. Correcting for the Influence of Frozen Lakes in Satellite Microwave Radiometer Observations through Application of a Microwave Emission Model. *Remote Sensing of Environment*, 115(12), 3695–3706.
- Luojuus, K., Pulliainen, J., Blasco Cutrona, A., Metsämäki, S. and Hallikainen, M. 2009. Comparison of SAR-based snow-covered area estimation methods for the boreal forest zone. *IEEE Geoscience and Remote Sensing Letters*, 6(3), 403–407.
- Metsämäki, S., Anttila, S., Huttunen, M. and Vepsäläinen, J. 2005. A feasible method for fractional snow cover mapping in boreal zone based on a reflectance model. *Remote Sensing of Environment*, 95(1), 77–95.
- Magagi, R. and Bernier, M. 2003. Optimal conditions for wet snow detection using RADARSAT SAR data. *Remote Sensing of Environment*, 84(2), 221–233.
- Nagler, T., and Rott, H. 2000. Retrieval of wet snow by means of multitemporal SAR data. *IEEE Transactions on Geoscience and Remote Sensing*, 38(2), 754–765.
- Pohjola, H. 2003. *Tutkaheijastuvuustekijän pystyjakauma Suomessa ja sen vaikutus tutkan sademittauksen tarkkuuteen*. Pro Gradu -tutkielma. University of Helsinki. In Finnish. (<http://ethesis.helsinki.fi/julkaisut/mat/fysik/pg/pohjola/>).
- Pulliainen, J. 2006. Mapping of snow water equivalent and snow depth in boreal and sub-arctic zones by assimilating space-borne microwave radiometer data and ground-based observations. *Remote Sensing of Environment*, 101(2), 257–269.
- Pulliainen, J., Grandell, J. and Hallikainen, M. 1999. HUT Snow Emission Model and its Applicability to Snow Water Equivalent Retrieval. *IEEE Transactions on Geoscience and Remote Sensing*, 37(3), 1378–1390.
- Rauste, Y., Lönnqvist, A., Molinier, M., Henry, J.-B. and Häme, T. 2007. Orthorectification and terrain correction of polarimetric SAR data applied in the ALOS/Palsar context. In: *Proc. IEEE International Geoscience and Remote Sensing Symposium*, 1618–1621.
- Rautiainen, K., Lemmetyinen, J., Pulliainen, J., Vehviläinen, J., Drusch, M., Kontu, A., Kainulainen, J. and Seppänen, J. L-Band Radiometer Observations of Soil Processes at Boreal and Sub-Arctic Environments. *IEEE Transactions on Geoscience and Remote Sensing*. (In press.)
- Shi, J., Dozier, J. and Rott, H. 1994. Snow mapping in alpine regions with synthetic aperture radar. *IEEE Transactions on Geoscience and Remote Sensing*, 32(1), 152–158.
- Trudel, M., Magagi, R. and Granberg, H. B. 2009. Application of target decomposition theorems over snow-covered forested areas. *IEEE Transactions on Geoscience and Remote Sensing*, 47(2), 508–512.

## Appendix I. Publications list

In the following the publications produced by the project personnel during the project are listed.

### Articles

- Gunn, G. E., Duguay, C. R., Derksen, Lemmetyinen, J. and Toose, P. 2011. Evaluation of the HUT modified snow emission model over lake ice using airborne passive microwave measurements. *Remote Sensing of Environment*, 115(1), 233–244.
- Kontu, A. and Pulliainen, J. 2010. Simulation of spaceborne microwave radiometer measurements of snow cover using in situ data and brightness temperature modelling. *IEEE Transactions on Geoscience and Remote Sensing*, 48(3), 1031–1044.
- Lemmetyinen, J., Derksen, C., Pulliainen, J., Strapp, W., Toose, P., Walker, A., Tauriainen, S., Pihlflyckt, J., Kärnä, J.-P. and Hallikainen, M. 2009. A Comparison of Airborne Microwave Brightness Temperatures and Snowpack Properties across the Boreal Forests of Finland and Western Canada. *IEEE Transactions on Geoscience and Remote Sensing*, 47(3), 965–978.
- Lemmetyinen, J., Pulliainen, J., Rees, A., Kontu, A., Qiu, Y. and Derksen, C. 2010. Multiple Layer Adaptation of HUT Snow Emission Model: Comparison with Experimental Data. *IEEE Transactions on Geoscience and Remote Sensing*, 48(4), 2781–2794.
- Lemmetyinen, J., Kontu, A., Kärnä, J.-P., Vehviläinen, J., Takala, M. and Pulliainen, J. 2011. Correcting for the Influence of Frozen Lakes in Satellite Microwave Radiometer Observations through Application of a Microwave Emission Model. *Remote Sensing of Environment*, 115(12), 3695–3706.
- Rautiainen, K., Lemmetyinen, J., Pulliainen, J., Vehviläinen, J., Drusch, M., Kontu, A., Kainulainen, J. and Seppänen, J. L-Band Radiometer Observations of Soil Processes at Boreal and Sub-Arctic Environments. *IEEE Transactions on Geoscience and Remote Sensing*. 2011.
- Takala, M., Luojus, K., Pulliainen, J., Derksen, C., Lemmetyinen, J., Kärnä, J.-P., Koskinen, J. and Bojkov, B. Estimating northern hemisphere snow water equivalent for climate research through assimilation of space-borne radiometer data and ground-based measurements. *Remote Sensing of Environment*, 115 (12), 3517–3529.. (In press.)

### Conference papers

- Antropov, O., Rauste, Y., and Häme, T. 2011. Multitemporal PolSAR for snow cover monitoring. In: *Proceedings of the 5th International Workshop on Science and Applications of SAR Polarimetry and Polarimetric Interferometry*, Frascati, Italy, 24–28 January 2011. ESA Special publication SP-695.
- Kärnä, J.-P., Huttunen, M., Metsämäki, S., Vehviläinen, B., Pulliainen, J., Lemmetyinen, J., Rauste, Y. and Berglund, R.. 2010. Improving hydrological forecasting using multi-source remote sensing data together with in situ measurements. In *Proceedings of IEEE 2010 International Geoscience and Remote Sensing Symposium (IGARSS 2010)*, Honolulu, Hawaii, July 25–30, 2010. pp. 1749–1752.

### Monographs

- Kärnä, J.-P. 2010. Using statistical inversion for the retrieval of geophysical parameters from the remote sensing data. Licentiate thesis. Aalto University School of Science and Technology. (<http://lib.tkk.fi/Lic/2010/urn013505.pdf>)
- Smolander, T. 2009. Lumen peittämän alan määrittäminen satelliittitulkalla. Kandidaatintutkielma. University of Helsinki. (In Finnish.)

### Presentations

- Kärnä, J.-P., Huttunen, M., Metsämäki, S., Vehviläinen, B., Pulliainen, J., Lemmetyinen, J., Kuitunen, T., Smolander, T., Rauste, Y., Berglund, R. and Perkola, P. Improving flood forecasting using multi-source remote sensing data and in situ measurements. 6th EARSeL Workshop: Cryosphere, Hydrology & Climate interactions, February 9th, 2011, Bern.
- Berglund, R., Toivanen, T., Rauste, Y., Vehviläinen, B., Kolhinen, V., Kärnä, J.-P., Lemmetyinen, J. and Pulliainen, J. A Presentation System for Flood Forecasting Products. Finnish remote sensing days 2011, November 24-25th, 2011, Espoo.

### Unpublished project reports

- Tulvaennustejärjestelmän vaatimusmäärittely, VTT, 19.4.2010
- Floodfore – Multisource flood prediction system - Prototype documentation, VTT, 31.8.2010
- Floodfore Prototype User Guide, VTT, 7.9.2010
- Kolhinen V. and Vehviläinen, B. 2011. Satellite observations of snow covered area and snow water equivalent in hydrological forecasts.

## DOCUMENTATION PAGE

<i>Publisher</i>	Finnish Environment Institute (SYKE)			<i>Date</i> April 2012
<i>Author(s)</i>	Juha-Petri Kärnä (editor), Vesa Kolhinen, Sari Metsämäki, Bertel Vehviläinen Timo Kuitunen, Juha Lemmetyinen, Jouni Pulliainen, Kimmo Rautiainen, Tuomo Smolander, Oleg Antropov, Robin Berglund, Jukka Kiviniemi, Yrjö Rauste			
<i>Title of publication</i>	<b>Improving flood forecasting using multi-source remote sensing data – Report of the Floodfore project</b>			
<i>Publication series and number</i>	The Finnish Environment 12/2012			
<i>Theme of publication</i>	Nature resources			
<i>Parts of publication/ other project publications</i>	The publication is available on the internet: <a href="http://www.ymparisto.fi/julkaisut">www.ymparisto.fi/julkaisut</a>			
<i>Abstract</i>	<p>The FloodFore project developed new methods to estimate hydrological parameters from multi source remote sensing and in situ data. The estimated parameters are important input to the watershed simulation model in order to improve the accuracy of the forecasts. Goal was also to develop and demonstrate a visualisation system for multi source information and to study the commercialization possibilities of the results of the project.</p> <p>Project was mainly funded by Tekes, but also several Finnish companies and two ministries (The Ministry of Transport and Communications and the Ministry of Agriculture and Forestry) participated in funding. The development work of the project was conducted in three institutes: Finnish Meteorological Institute, Finnish Environment Institute and VTT Technical Research Centre of Finland. These institutes also participated in funding of the project.</p> <p>The main achievements of the project are:</p> <ul style="list-style-type: none"> <li>- Development and validation of a satellite based snow water equivalent (SWE) estimation method for the area of Finland. Method was taken into operative use at SYKE where watershed simulation model uses the SWE estimates.</li> <li>- Development of a weather radar based accumulated precipitation estimation method. Method estimates the accumulated 24 hour precipitation using weather radar and precipitation gauges together. Method was taken into operational use.</li> <li>- Determination of soil freezing state from the satellite observations</li> <li>- Testing the benefit of the remote sensing products to the hydrological forecasting</li> <li>- Method to estimate snow water equivalent at high spatial resolution using both microwave radiometer and SAR data</li> <li>- Development and demonstration of a visualisation system for multi source information</li> <li>- Study of the commercialisation possibilities of the project results</li> </ul>			
<i>Keywords</i>	floods, remote sensing, snow, SWE, precipitation, frost			
<i>Financier/ commissioner</i>	Finnish Environment Institute (SYKE)			
	ISBN	ISBN 978-952-11-4001-3 (PDF)	ISSN	ISSN 1796-1637 (on-line)
	<i>No. of pages</i> 46	<i>Language</i> English	<i>Restrictions</i> Public	<i>Price (incl. tax 8 %)</i> -
<i>For sale at/ distributor</i>	Finnish Environment Institute (SYKE) P.O.Box 140, FI-00251 Helsinki, Finland Tel. +358 20 610 123, fax +358 20 490 2190 Email: <a href="mailto:neuvonta.syke@ymparisto.fi">neuvonta.syke@ymparisto.fi</a> , <a href="http://www.environment.fi/syke">www.environment.fi/syke</a>			
<i>Financier of publication</i>	Finnish Environment Institute (SYKE) P.O.Box 140, FI-00251 Helsinki, Finland Tel. +358 20 610 123, fax +358 20 490 2190 Email: <a href="mailto:neuvonta.syke@ymparisto.fi">neuvonta.syke@ymparisto.fi</a> , <a href="http://www.environment.fi/syke">www.environment.fi/syke</a>			
<i>Printing place and year</i>				

## KUVAILEHTI

Julkaisija	Suomen ympäristökeskus (SYKE)			Julkaisu-aika April 2012
Tekijä(t)	Juha-Petri Kärnä (toimittaja), Vesa Kolhinen, Sari Metsämäki, Bertel Vehviläinen Timo Kuitunen, Juha Lemmetyinen, Jouni Pulliainen, Kimmo Rautiainen, Tuomo Smolander, Oleg Antropov, Robin Berglund, Jukka Kiviniemi, Yrjö Rauste			
Julkaisun nimi	<b>Improving flood forecasting using multi-source remote sensing data – Report of the Floodfore project</b>			
Julkaisusarjan nimi ja numero	Suomen ympäristö 12/2012			
Julkaisun teema	Luonnonvarat			
Julkaisun osat/ muut saman projektin tuottamat julkaisut	Julkaisu on saatavana ainoastaan internetistä: <a href="http://www.ymparisto.fi/julkaisut">www.ymparisto.fi/julkaisut</a>			
Tiivistelmä	<p>FloodFore-projektissa kehitettiin uusia menetelmiä hydrologisten suureiden määrittämiseen monilähteisestä kaukokartoitus- sekä in situ -havainnoista. Määritetyt suuret ovat vesistömallin kannalta tärkeitä, jotka pystyvät parantamaan mallin ennusteiden tarkkuutta. Tavoitteina oli myös kehittää ja demonstroida monilähteisen tiedon visualisointijärjestelmä sekä selvittää projektin tulosten kaupallistamismahdollisuuksia.</p> <p>Projektin rahoitti pääosin Tekes, mutta mukana oli myös useita suomalaisia yrityksiä sekä kaksi ministeriötä (Liikenne ja viestintä- sekä Maa- ja metsätalousministeriö). Projektin kehitystyö tehtiin kolmessa tutkimuslaitoksessa: Ilmatieteen laitos, Suomen ympäristökeskus sekä VTT. Nämä laitokset myös osallistuivat projektin rahoitukseen.</p> <p>Projektin pääsaavutukset olivat seuraavat:</p> <ul style="list-style-type: none"> <li>- Satelliittipohjaisen lumen vesiarvon määrittämismenetelmän kehittäminen ja validointi Suomen alueelle. Menetelmä otettiin operatiiviseen käyttöön SYKE:n vesistömallin syötteenä.</li> <li>- Sääntökammitauksiin perustuvan kumulatiivisen sadannan määrittämismenetelmän kehitys. Menetelmällä määritetään kumulatiivinen vuorokausisadanta sääntökammitauksien ja sademittarien yhteiskäytöllä. Menetelmä on otettu operatiiviseen käyttöön.</li> <li>- Maan routaantumishetken määrittäminen satelliittihavainnoista.</li> <li>- Satelliittihavaintojen hyödyn arviointi vesistömallin ennustustarkkuudelle.</li> <li>- Menetelmä lumen vesiarvon määrittämiseksi suurella spatiaalisella erotuskyvyllä käyttäen yhdessä satelliitista tehtyjä mikroaaltoradiometri- ja tutkahavaintoja.</li> <li>- Monilähteisen tiedon visualisointijärjestelmän prototyypin kehittäminen ja demonstrointi.</li> <li>- Projektin tulosten kaupallistamismahdollisuuksien selvittäminen.</li> </ul>			
Asiasanat	tulvat, kaukokartoitus, lumi, lumen vesiarvo, sadanta, routa			
Rahoittaja/ toimeksiantaja	Suomen ympäristökeskus			
	ISBN	ISBN 978-952-11-4001-3 (PDF)	ISSN	ISSN 1796-1637 (verkkokj.)
	Sivuja 46	Kieli english	Luottamuksellisuus julkinen	Hinta (sis.alv 8 %) -
Julkaisun myynti/ jakaja	Suomen ympäristökeskus (SYKE) PL 140, 00251 HELSINKI Puh. 020 610 123 Sähköposti: <a href="mailto:neuvonta.syke@ymparisto.fi">neuvonta.syke@ymparisto.fi</a> , <a href="http://www.ymparisto.fi/syke">www.ymparisto.fi/syke</a>			
Julkaisun kustantaja	Suomen ympäristökeskus (SYKE) PL 140, 00251 HELSINKI Puh. 020 610 123 Sähköposti: <a href="mailto:neuvonta.syke@ymparisto.fi">neuvonta.syke@ymparisto.fi</a> , <a href="http://www.ymparisto.fi/syke">www.ymparisto.fi/syke</a>			
Painopaikka ja -aika				

## PRESENTATIONSBLAD

<i>Utgivare</i>	Finlands miljöcentral (SYKE)			<i>Datum</i> April 2012
<i>Författare</i>	Juha-Petri Kärnä (red.), Vesa Kolhinen, Sari Metsämäki, Bertel Vehviläinen Timo Kuitunen, Juha Lemmetyinen, Jouni Pulliainen, Kimmo Rautiainen, Tuomo Smolander, Oleg Antropov, Robin Berglund, Jukka Kiviniemi, Yrjö Rauste			
<i>Publikationens titel</i>	<b>Improving flood forecasting using multi-source remote sensing data – Report of the Floodfore project</b>			
<i>Publikationsserie och nummer</i>	Miljön i Finland 12/2012			
<i>Publikationens tema</i>	Naturtillgångar			
<i>Publikationens delar/ andra publikationer inom samma projekt</i>	Publikationen finns endast på internet: <a href="http://www.ymparisto.fi/julkaisut">www.ymparisto.fi/julkaisut</a>			
<i>Sammandrag</i>	<p>I projektet FloodFore utvecklades nya metoder för bestämning av hydrologiska variabler med hjälp av data från flera fjärranalys- och in situ -observationskällor. Huvudvikten låg på variabler som kunde tänkas bidra till bättre noggrannhet i de hydrologiska modellprognoserna. Inverkan av två variabler, snötäckets vattenvärde och den snötäckta arealen, testades. I samband med projektet utvecklades och demonstrerades också ett visualiseringssystem för information från många källor. Dessutom utreddes möjligheterna till kommersiellt utnyttjande av projektresultaten.</p> <p>Projektet finansierades huvudsakligen av Tekes, men även flera finländska företag samt två ministerier (kommunikationsministeriet samt jord- och skogsbruksministeriet) bidrog med finansiering. Utvecklingsarbetet skedde vid tre forskningsinstitut: Meteorologiska institutet, Finlands miljöcentral samt VTT. Även dessa bidrog till finansieringen.</p> <p>De huvudsakliga resultaten:</p> <ul style="list-style-type: none"> <li>- Utveckling och validering av en satellitbaserad metod för bestämning av snötäckets vattenvärde inom Finlands territorium. Metoden har tagits i operativt bruk som input till SYKEs hydrologiska modell.</li> <li>- Utveckling av en väderradarbaserad metod för bestämning av kumulativ nederbörds mängd. Metoden går ut på att de kumulativa dygnsvärdena av nederbörd beräknas utgående från väderradarmätningar och regnmätarresultat. Metoden har tagits i operativt bruk.</li> <li>- Bestämning av tidpunkten för tjälbildning utgående från satellitobservationer.</li> <li>- Bedömning av nyttan av satellitobservationerna gällande noggrannheten i de hydrologiska modellprognoserna.</li> <li>- En metod för bestämning av snötäckets vattenvärde med stor spatiell resolution genom kombinerad användning av satellitbaserade mikrovågsradiometer- och radarobservationer.</li> <li>- Utveckling och demonstrering av en prototyp för ett visualiseringssystem för information från många källor.</li> <li>- Utredning av möjligheterna att kommersiellt utnyttja resultaten.</li> </ul>			
<i>Nyckelord</i>				
<i>Finansiär/ uppdragsgivare</i>	Finlands miljöcentral (SYKE)			
	ISBN	ISBN 978-952-11-4001-3 (PDF)	ISSN	ISSN 1796-1637 (online)
	<i>Sidantal</i> 46	<i>Språk</i> Engelska	<i>Offentlighet</i> Offentlig	<i>Pris (inneh. moms 8 %)</i> -
<i>Beställningar/ distribution</i>	Finlands miljöcentral (SYKE) PB 140, 00251 Helsingfors Tfn. +358 20 610 123 Epost: <a href="mailto:neuvonta.syke@ymparisto.fi">neuvonta.syke@ymparisto.fi</a> , <a href="http://www.miljo.fi/syke">www.miljo.fi/syke</a>			
<i>Förläggare</i>	Finlands miljöcentral (SYKE) PB 140, 00251 Helsingfors Tfn. +358 20 610 123 Epost: <a href="mailto:neuvonta.syke@ymparisto.fi">neuvonta.syke@ymparisto.fi</a> , <a href="http://www.miljo.fi/syke">www.miljo.fi/syke</a>			
<i>Tryckeri/tryckningsort och -år</i>				



Current remote sensing satellites can provide valuable information relevant to hydrological monitoring. And by using available in situ measurements together with the satellite data the information can be even more valuable.

The FloodFore project developed new methods to estimate hydrological parameters from multi source remote sensing and in situ data. These hydrological parameters are important input to the watershed simulation model in order to improve the accuracy of its forecasts.

In the project several new methods were either developed or demonstrated: satellite based snow water equivalent (SWE) estimation, weather radar based accumulated precipitation estimation, satellite based soil freezing state determination, and SWE estimation with high spatial resolution using both microwave radiometer and SAR data. Also a visualisation system for multi source information was developed to demonstrate the new products to users.

The effect of the snow remote sensing estimates to the hydrological forecasting accuracy was studied for the Kemijoki river basin.

The commercialisation possibilities of the results of the project were also studied.

